Recent Advances in Variable Flux Memory Machines for Traction Applications: A Review

Hui Yang, Heyun Lin and Z. Q. Zhu

(Invited)

***Abstract*—This paper overviews the recent advances in variable flux memory machines (VFMMs) for traction applications with particular reference to newly emerged machine topologies and related control strategies. Due to the use of flux memorable low coercive force (LCF) magnets, the air-gap flux of VFMM can be flexibly varied via a magnetizing current pulse. Thus, the copper loss associated with the flux weakening current and high-speed iron loss can be significantly reduced, and hence high efficiency can be achieved over a wide speed and torque/power operation. These merits make VFMM potentially attractive for electric vehicle (EV) applications. Various novel VFMMs are reviewed with particular reference to their topologies, working principle, characteristics and related control techniques. In order to tackle the drawbacks in the existing VFMMs, some new designs are introduced for performance improvement. Then, the electromagnetic characteristics of an exemplified EV-scaled switched flux memory machine and various benchmark traction machine choices, such as induction machine, synchronous reluctance machines, as well as commercially available Prius 2010 interior permanent magnet (IPM) machine are compared. Finally, the key challenges and development trends of VFMM are highlighted, respectively.**

***Index Terms*—AC-magnetized, DC-magnetized, electrical machines, electric vehicles, hybrid permanent magnet (PM), memory machine, variable flux.**

I. Introduction

A. Background and Motivation

DUE TO the merits of high torque density and high efficiency, permanent magnet (PM) machine is extensively recognized as a promising candidate for traction applications, such as electric vehicle (EV) [1]-[6]. Nevertheless, the non-adjustable air-gap flux is a major concern for the conventional PM machines equipped with rare-earth magnets. This will result in a limited constant-power speed range (CPSR), if no special countermeasure is taken. Conventionally, the *d*-axis flux-weakening (FW) current [7] is utilized to counteract the PM fields for speed range extension. However, due to the inverter limitations in terms of current and voltage ratings, the speed range and the operating efficiency of conventional PM machines may still be inadequate for EV requirements. Meanwhile, the *d*-axis FW armature reaction magneto motive forces (MMFs) normally pose a potential demagnetization risk on PMs [2]. Besides, the resultant excitation copper loss associated with FW current leads to the reduction of the overall driving cycle operating system efficiency, which is undesirable for traction applications. As a whole, the conventional PM machines generally suffer from the conflicted low-speed high torque and high-speed high power capabilities. From this viewpoint, it is desirable to control the MMF of permanent magnets according to the specific requirement at different speeds [3].

Recently, the concept of "variable flux memory machine (VFMM)" [8] has been proposed to achieve "true" wide speed operation. The flexible air-gap flux adjustment can be achieved by applying a current pulse to either remagnetize or demagnetize low coercive force (LCF) PMs. Consequently, their magnetization state (MS) can be "memorized" by a specific current pulse level, allowing FW control current to be greatly reduced and the corresponding losses are minimized. This is similar to the variable flux characteristic of induction machines and wound-field synchronous machines.

The motivation of VFMMs is to combine high torque density of conventional constant PM flux machine with variable PM flux characteristics for manipulating losses [10]-[13]. Since the associated excitation copper loss is negligible during the MS control, high efficiency can be maintained within a wide operating range. In addition, since back electromotive force (EMF) of the machine can be controlled due to the variable flux property so that the inverter failure under high-speed operation can be well prevented. Meanwhile, the CPSR can be further extended within the inverter voltage constraint by purposely demagnetizing the LCF PMs. The abovementioned distinct merits make VFMM a promising candidate for traction applications. In fact, variable flux machines have been

This article was submitted for review on 13, March, 2018.

This work was jointly supported in part by National Natural Science Foundations of China under Grant 51377036 and 51377020, in part by Natural Science Foundation of Jiangsu Province for Youth (BK20170674), in part by Specialized Research Fund for the Doctoral Program of Higher Education of China (20130092130005), and in part by the Fundamental Research Funds for the Central Universities (2242017K41003). The first author would like to specially thank Prof. Z. Q. Zhu's guidance and encouragement during the one-year joint studentship at The University of Sheffield, which is financially supported by the China Scholarship Council. The authors would like to thank their colleagues at Southeast University, China, in particular the contributions made by Dr. Dong Wang, Mr. Erxing Zhuang, Mr. Ling Qin, and Mr. Shukang Lyu.

Hui Yang and Heyun Lin are with School of Electrical Engineering, Southeast University, Nanjing, P. R. China (e-mail: *huiyang@seu.edu.cn, hyling@seu.edu.cn).

Z. Q. Zhu is with Department of Electronic and Electrical Engineering, University of Sheffield, Sheffield, U.K. (z.q.zhu@sheffield.ac.uk).

successfully commercialized in duty-cycle based application such as washing machines [16]. In the last decade, VFMMs have experienced rapid technical advancements, and received growing research interests by many scholars and EV manufacturers worldwide [8]-[75].

Generally, the existing VFMMs can be divided into AC- [8]-[37] and DC-magnetized types [38]-[75] according to the current pulse pattern. Furthermore, the AC-magnetized VFMM employs stator armature winding to produce *d*-axis current pulse with resorting to the vector control. The benefits of using armature windings are simple structure similar to the conventional PM machines, as well as less circuit components and cost. However, the drawbacks are high requirements on the armature winding and inverter rating. Furthermore, the AC-magnetized VFMM can be sub-categorized into two types, which are variable flux [8]-[32] and pole-changing [33]-[37], respectively. Further, the variable flux topologies can be divided into series and parallel magnetic circuit types. On the other hand, DC-magnetized VFMM can be classified into stator-PM [38]-[65][68]-[74], rotor-PM [66][67] and dual-sided PM structures [75] based on the PM location. The overall categorization of the existing VFMMs is illustrated in Fig. 1.

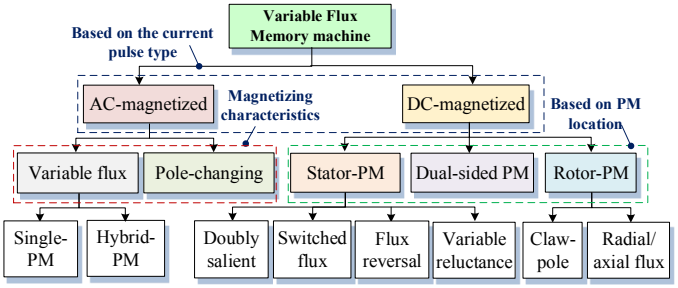

Fig. 1. Categorization of variable flux memory machines.

B. Organization of This Review

This paper reviews the recent development of VFMM, which can be organized as follows: in Section II, the VF principle and basic features of VFMM are described in the potential context of EV applications. In addition, in Sections III and IV, various novel AC- and DC-magnetized VFMMs are reviewed with particular reference to their topologies, working principles, characteristics and related control strategies. In order to deal with the drawbacks in the existing VFMMs, some new designs are introduced for performance improvement in Section V. This is followed by a comparison of electromagnetic characteristics of an EV-scaled switched flux memory machine and various benchmark traction machines, such as induction machine, synchronous reluctance machines, as well as Prius 2010 interior permanent magnet (IPM) machine in Section VI. Finally, the key challenges and development trends of VFMMs are highlighted in Section VII.

II. Variable Flux Principle

A. Invention of VFMM Concept

The concept of the "VFMM" was firstly proposed by V. Ostovic [8]. As shown in Fig. 2, a spoke-type IPM machine with a sandwiched rotor is converted into a VFMM by using tangential LCF PMs. The VF property is achieved by applying *d*-axis current in the stator windings and partially reversing the magnetization direction of the magnet portion close to the shaft, which is thinner and more vulnerable to the demagnetization MMF. Consequently, the PM fluxes close to air-gap are largely short-circuited, allowing the FW effect. Meanwhile, the required FW control current and hence the corresponding copper losses are significantly reduced. The magnetizing physics and hybrid PM topology are analyzed in detail in [9] and [10].

B. Nonlinear Hysteresis Property of LCF PMs

The VF principle of VFMM can be represented by a simplified illustration of the hysteresis model of LCF PMs as shown in Fig. 3. It can be observed that the coercive force of LCF PM is relatively low, which equals to 1/6~1/3 of that of NdFeB. This enables the possibility of flexible movement of the operating points along different recoil lines when applying an external magnetizing MMF. For instance, the working point of the PM is initiated at P_1, which is the cross point of the load line and the demagnetizing curve. When applying a demagnetizing current pulse, the working point will descend to *G*. After the withdrawal of the current pulse, the working point will move along a new recoil line and stabilize at new working point P_2. On the other hand, when a remagnetizing current pulse is applied, the working point of the PM will track the trajectory of *CDEB* and return to P_1.

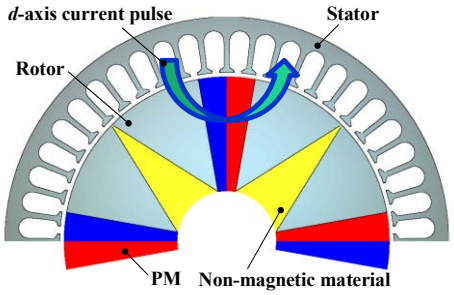

Fig. 2. Topology of the original variable flux memory machine [8].

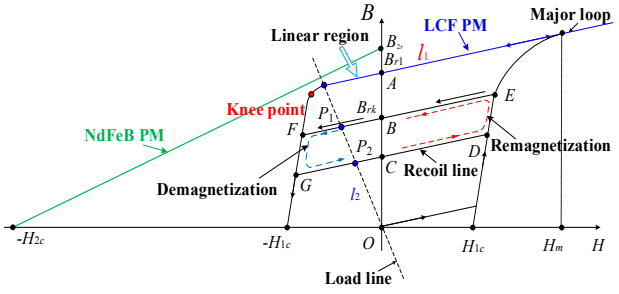

Fig. 3. Simplified illustration of hysteresis model of LCF PM.

Obviously, the serious hysteresis nonlinearity inevitably makes the relationship between the MS of magnet and the magnetizing current pulses complicated, which is identified as one major challenge for analyzing VFMMs. Therefore, various numerical hysteresis models are employed to characterize the repetitive hysteresis behavior of LCF PM, such as piecewise linear model [38], Presaich [42], and Frolich models [50], etc.

These models are usually coupled with finite element method (FEM) to compute the specific working point of each PM element considering the hysteresis property. However, it is still very challenging to accurately predict the working point of LCF PM due to the highly nonlinear hysteresis models.

To reduce the required magnetizing current from the stator windings to a reasonable amount, AlNiCo magnets are widely used in VFMM due to their LCF attribute. In addition, this magnet material has a relatively high remanence flux density and a high Curie temperature of 700~850°C, which is preferable when designing for high torque density and low magnetizing current. However, the very low coercive force makes this type of machine prone to demagnetization under load current, and hence designing for high torque density is quite challenging.

The alternative magnet materials can be utilized in VFMM, e.g. Ferrite and SmCo PMs, and their typical hysteresis models are illustrated in Fig. 4. Ferrite has a wide linear region and an acceptable coercivity (210~400kA/m), but the low thermal stability and remanence are adverse to the dynamic performance improvement. The VFMMs developed by Japan EV companies use SmCo PMs instead of AlNiCo magnets, since its more linear hysteresis nature allows the precise control of MS (including intermediate levels) to be more readily achieved [11]. Besides, due to high Curie temperature (~720°C), high residual flux density (0.8~1.0T) and acceptable coercivity (160~300kA/m), SmCo is believed to provide high torque production and stable MS in the cases of heavy loads.

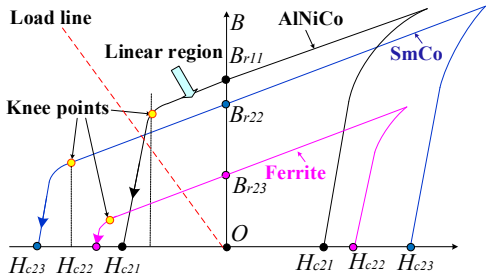

Fig. 4. Typical hysteresis curves of LCF magnet choices.

C. Potential Advantages for EV Duty-cycle Based Operation

In order to clearly illustrate the potential advantages of VFMM for EVs, the typical torque/power-speed characteristics required for traction applications are illustrated in Fig. 5(a). It implies that traction machines are desired to provide high torque for starting, at low speeds and hill climbing, and high power as well as wide CPSR for high-speed cruising. Besides, high efficiency over wide speed and torque ranges, particularly under low torque operation which are frequently operating region of NEDC and WLTC driving cycles [13].

The VF property of VFMM allows high speed operation without requiring continuous FW current, which may cause significant additional copper losses. In general, the variable PM flux linkage is an additional degree of freedom for the loss minimization. The resultant typical torque/power-speed curves of VFMM are plotted in Fig. 5(b). It demonstrates that the overall efficiency over a driving cycle can be improved compared to the conventional PM machines by dynamically controlling the PM flux linkage. This is mainly attributed to the fact that the peak power and the high efficiency distribution patterns of VFMM vary significantly at different MSs.

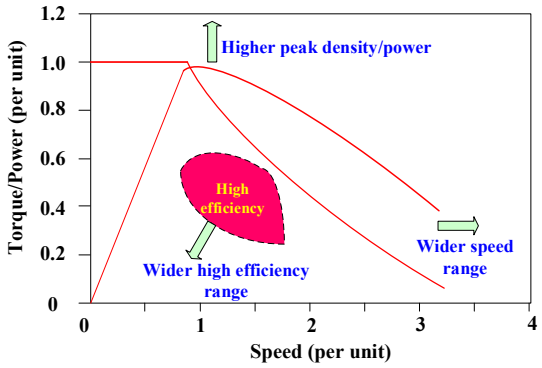

(a)

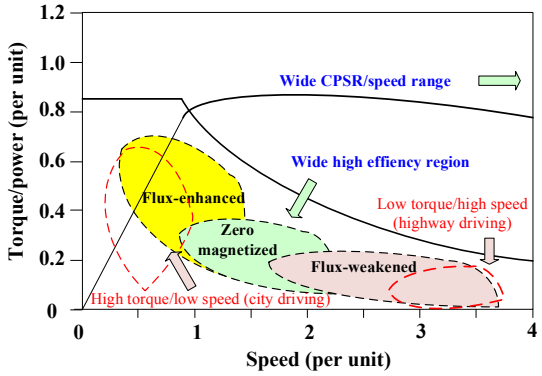

(b)

Fig. 5. Illustration of machine operating areas for EV duty cycle. (a) EV traction machine requirement. (b) VFMM.

The FW performance improvement with VFMM design can be clearly illustrated as follows. When the terminal voltage and phase current reach the inverter limits, i.e., all the current is converted to the negative d-axis flux-weakening component [1], the maximum achievable speed $\omega_{\max}$ can be expressed as

$$\omega_{\max}=\frac{u_{\lim}}{N_r\left(\Psi_{\max}-k_m\left(1-\frac{1}{\alpha_{mag}}\right)\Psi_{\max}-L_d i_{\lim}\right)} \tag{1}$$

where u_{lim}, i_{lim}, L_d, and N_r are the maximum phase voltage, phase current, d-axis inductance and rotor pole number; k_m denotes the LCF magnetizing ratio between 0 and 1; Ψ_{max} is the maximum phase flux-linkage. The flux adjusting ratio α_{mag} for indicating the maximal achievable variable speed range can be defined as the ratio of the flux linkage under the flux-enhanced and flux-weakened states

In addition, the base speed ω_{base}, which stands for the dividing point between the constant-torque and constant-power operating regions, can be expressed by

$$\omega_{base}=\frac{u_{\lim}}{N_r\sqrt{\left(\Psi_{\max}-k_m\left(1-\frac{1}{\alpha_{mag}}\right)\Psi_{\max}\right)^2+\left(L_q i_{\lim}\right)^2}} \tag{2}$$

where L_q stands for the q-axis inductance. Besides, a flux-weakening factor k_{fw} that indicates the capability extending the speed range above the base speed can be defined as

$$k_{fw} = \frac{L_d i_{\lim}}{\Psi_{\max} - k_m\left(1 - \frac{1}{\alpha_{mag}}\right)\Psi_{\max}} \quad (3)$$

As a result, it can be derived from (1)~(3), a wider achievable speed range and a better FW capability can be obtained by demagnetizing LCF PMs, which theoretically confirms the advantages of VFMM for EV applications.

III. AC-MAGNETIZED VFMM

Since the original "VFMM" (see Fig. 2) was proposed by V. Ostovic [8], various VFMM topologies [9]-[75] based on the conventional IPM structures have been reported, which employ armature winding to energize a *d*-axis current pulse to achieve online MS manipulation. Without loss of generality, the existing AC-magnetized VFMM can be designed and implemented as either variable flux [8]-[32] or pole changing [33]-[37] types.

A. Variable Flux Type

1) Single-PM

For the conventional VFMMs featuring "L_d<L_q", a negative *d*-axis current is normally utilized to achieve the maximum-torque-per-ampere (MTPA) control. Under these circumstances, it is difficult to avoid unintentional demagnetization so that the PM flux linkage cannot be fully utilized. Accordingly, in order to fully use PM flux linkage, a combined concept of flux intensified (FI) machine and variable flux property has been proposed recently, i.e., a flux intensifying VFMM (FI-VFMM) characterized by a reversed saliency "L_d>L_q" [11]-[16] [20]-[24].

The FI structure has three main advantages for VFMM design: First, the MS of the LCF PM can be well preserved when a positive FW current is employed to permit positive reluctance torque production. Secondly, sufficient power conversion capability is maintained while reducing the use of expensive rare earth materials, such as dysprosium. Thirdly, the proposed machine is designed to have a torque-speed envelope with a wider CPSR, while reducing the losses typically resulting from high speed FW operation. The topology and the prototype of typical FI-VFMM [11] are shown in Fig. 6. A flux leakage path is designed for energy loss reduction over load cycles, wider magnetic flux adjusting range, and beneficial self-sensing property.

In a similar way, the flux-concentrated FI-VFMM designs are proposed in [20] and [23], as shown in Fig. 7. This topology with a spoke PM and a fractional-slot winding configuration is further investigated. The design suggestions are provided in [22] to reduce the magnetizing current and inverter rating, in particular by making the tooth width larger and optimizing magnet dimensions, using non-magnetic materials for flux barriers as well as modified rotor bridge structures.

In terms of control aspects for FI-VFMM, to avoid the pulsating torque during MS change, the MS manipulation can be implemented at zero speed, zero load condition by using voltage disturbance state filter to correct the estimates from a flux observer [12]. With this control method, the machine torque is accurately estimated, and the torque ripple (due to reluctance torque) during MS change is minimized with a decoupling i_q control. In this work, the pulsating torque ripple is minimized, but MS manipulation is established only at low speeds and the voltage limitations have not been investigated. As shown in Fig. 8, a hysteresis-based MS selection control is proposed in [12] to choose the MS manipulation timing in a reasonable manner over a duty-cycle operation to reduce the operational loss by balancing the transient and steady-state energy consumptions.

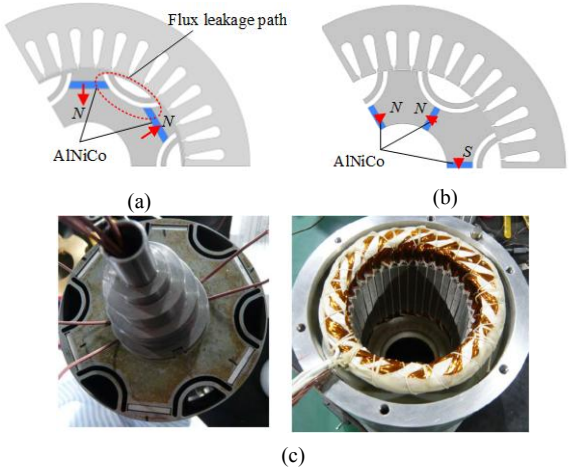

Fig. 6. FI-VFMMs equipped with (a) radially magnetized magnets and surface iron bridge, as well as (b) circumferentially magnetized magnets. (c) Prototype.

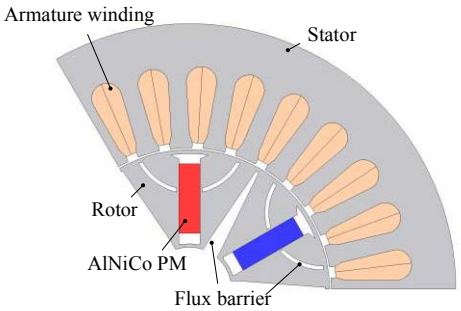

Fig. 7. FI-VFMMs with spoke-type AlNiCo PMs.

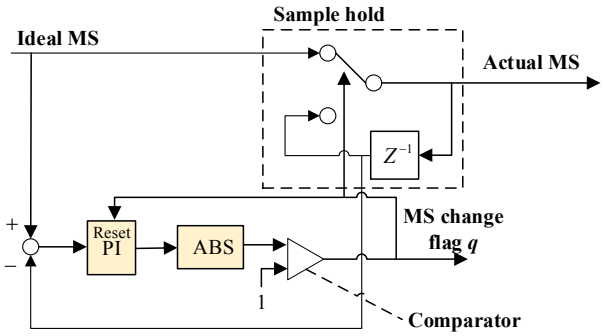

Fig. 8. A hysteresis-based MS selection control for FI-VFMM.

The artificial neural network based MTPA control scheme for the spoke-type FI-VFMM is implemented in [21]. With this method, the control effort is significantly simplified by reducing the effect of the inductance nonlinearity under MS manipulation operation. Meanwhile, the on-load transient response of torque and speed is further improved with a MS

controller which eliminates the influences of the system parameter variations. In addition, a modified adaptive nonlinear filter (MANF) is proposed as shown in Fig. 9 to realize the magnetic flux linkage estimation and the online close-loop MS control [24].

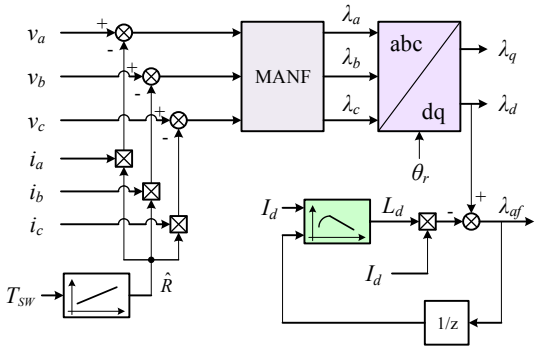

Fig. 9. A modified adaptive nonlinear filter based flux linkage estimation control for FI-VFMM.

2) Hybrid-PM

a) Parallel PM type

A hybrid variable-magnetic-force motor was proposed by Prof. K. Sakai et al [18]. The radially magnetized NdFeB PMs act as a constant MMF source whilst the tangentially magnetized AlNiCo PMs serve as a flux regulator. The cross-coupling demagnetization phenomenon of this machine is identified and investigated in [25]. It is found that the unintentional demagnetization of the LCF PM occurs particularly under loaded operation due to the cross-coupling effect. Therefore, various improved hybrid-PM structures are proposed and investigated by using *q*-axis barriers. A hybrid-PM VFMM with "V"-shape NdFeB PMs close to the shaft is presented [25]. The cross-coupling demagnetization effect is decreased by introducing two air barriers at the two sides of LCF PMs. Besides, Ferrite magnet is employed instead of commonly used AlNiCo PM to further improve the on-load demagnetization withstand capability and obtain more linear magnetizing characteristics.

b) Series PM type

In order to resolve the drawbacks of the previous FI-VFMMs in terms of limited torque density and power maintaining capability at high speeds, a series hybrid-PM FI-VFMM is proposed [27], as illustrated in Fig. 10. The rotor has a salient pole type topology with large *q*-axis flux barriers so as to minimize leakage flux and effectively utilize the stator induced magnetic flux linkage for magnetization. In addition, the feasibility of series and parallel hybrid-PM arrangements in FI-VFMM is investigated. It is found that both configurations help to improve the torque density, only the series configuration can help to improve the high speed power capability, which can well meet the EV requirement. In addition, an improved flux observer is proposed for the series hybrid-PM FI-VFMM prototype to estimate the MS based on the structured neural network (SNN) instead of the conventional look-up table method [28][29]. The SNN is utilized to describe the relationship between the inductance and current under different MS cases, resulting in a data filing space saving and an accurate PM flux linkage identification.

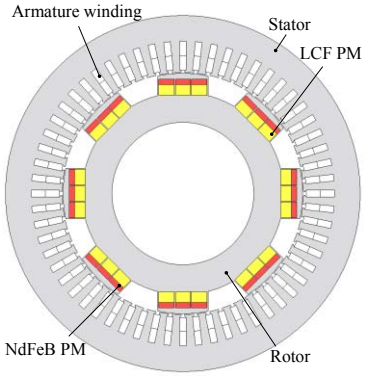

Fig. 10. Series hybrid-PM FI-VFMM.

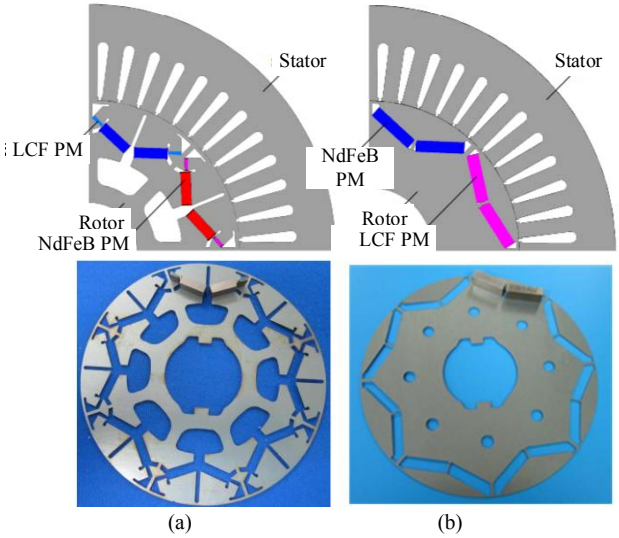

Fig. 11. Hybrid-PM VFMM based on Prius 2010 IPM machine. (a) Parallel-type. (b) Series-type.

A series hybrid-PM VFMM based on the Prius 2010 PM structure is proposed in [30], in which the NdFeB PMs and the LCF PM alternatively form different PM poles. With this design, the unintentional demagnetization caused by armature reaction are well prevented. Meanwhile, the reluctance torque can be effectively utilized to improve the torque density due to the positive magnetizing effect of the NdFeB magnet acting on the LCF PMs. In addition, the electromagnetic characteristics of series and parallel hybrid-PM VFMMs (see Fig. 11) are compared [31][32]. It demonstrates that the series-type exhibits higher torque density than its parallel counterpart, but suffers from evident unipolar end effect due to the unbalanced magnetic pole arrangement [31]. On the other hand, the LCF PMs of the parallel-type VFMM suffers from severe unexpected demagnetization risk particularly under heavy loaded operation.

B. Pole-Changing Type

As the polarities of variable-flux magnets can be flexibly adjusted, the AC-magnetized VFMM having rotor-PM topologies can be also implemented as a pole-changing machine by reconfiguring the magnetic flied distributions. The concept of "pole-changing (PC)" was firstly introduced by V. Ostovic by using VFMM principle to change the magnetization

directions of specific pieces of LCF magnets [33]. Two sets of windings are employed to enable the pole-changing operation. Thus, the PM pole number can be varied based on the performance requirements under different operating regions as shown in Fig. 12, such as higher pole number for high torque output at low speeds, while lower pole number for wide CPSR and high efficiency at low loads.

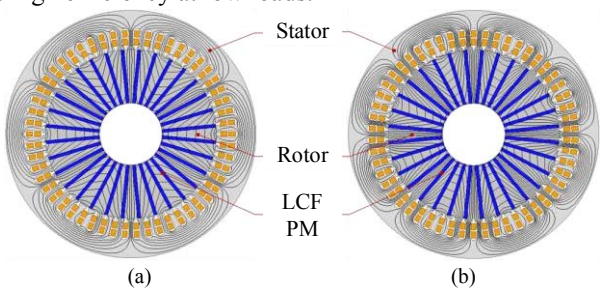

Fig. 12. Original pole-changing VFMM. (a) 6-pole mode. (b) 8-pole mode.

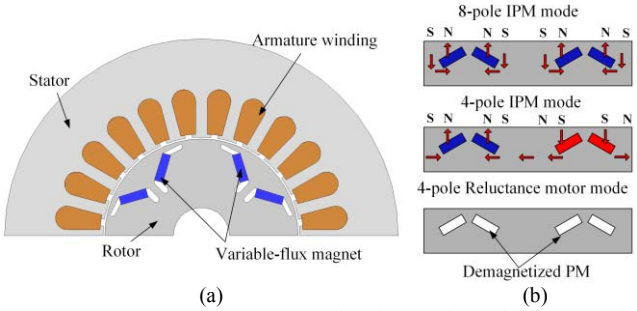

Fig. 13. PCMM structure. (a) Cross-sectional view. (b) Embodiment of three different pole modes.

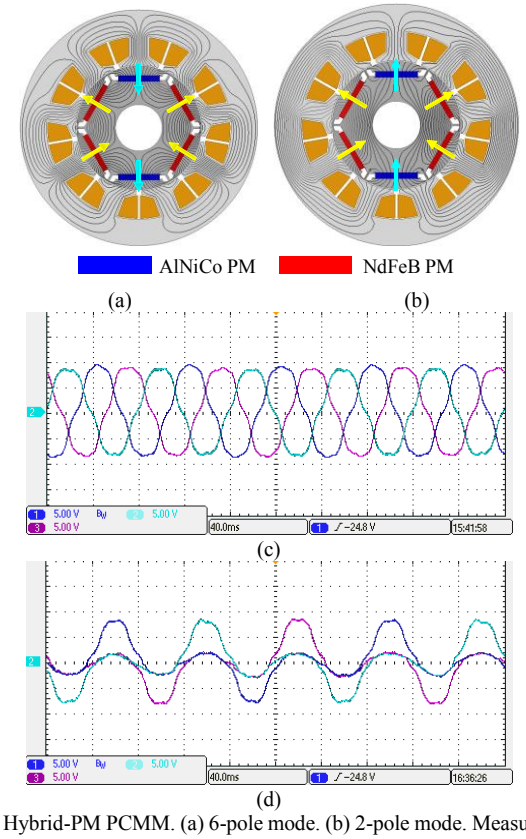

Fig. 14. Hybrid-PM PCMM. (a) 6-pole mode. (b) 2-pole mode. Measured EMF waveforms under (c) 6-pole mode. (d) 2-pole mode.

Similarly, Prof. K. Sakai proposes a pole-changing MM (PCMM) with three torque modes that can change the number of poles and produce three different types of torque [34]. The machine topology and operating principle are illustrated in Fig. 13. In low-speed range, the PCMM operates as a "V"-shaped 8-pole machine and produces a high PM torque. In the intermediate speed range, the PCMM acts as a 4-pole IPM machine delivering both reluctance and PM torques. Under high speed operation, the PCMM becomes a 4-pole reluctance machine. It should be noted that the armature winding connection should be changed corresponding to the number of poles. This type of PCMM enables the induced voltage to vary from 53% to 100%.

In addition, the PCMMs with different hybrid PM arrangements are proposed as shown in Fig. 14 , which possesses "6-2 pole" switching capability [35]-[37]. This machine is equipped with a fractional-slot concentrated winding having simple winding connection in both 6 pole-mode and 2-pole mode. The cogging torque optimization is performed by combined numerical methods in [37] to improve the torque quality at 2-pole mode. The machine structure, manufactured prototype and tested back-EMF waveforms are shown in Fig. 13, which confirm the effectiveness of the "pole-changing" operation.

IV. DC-Magnetized VFMM

The DC-magnetized VFMM employs additional DC magnetizing coils to magnetize/demagnetize the LCF magnets. The benefit of this configuration is that the armature and magnetizing windings can be controlled independently. The requirements on armature windings and converter can be greatly reduced. However, additional windings and converter are required, and the machine structures are generally more complicated.

A. Stator-PM Type

1) Doubly Salient

A doubly-salient (DS) VFMM (DS-VFMM) is proposed by incorporating the concept of "flux-memory" into a stator-PM machine having DS and outer-rotor configuration [38] [39]. The topologies using single-PM and dual-PM [40] are illustrated in Figs. 15(a) and (b), respectively. It can be seen that the DS-VFMMs have a double-layer stator with 5-phase armature windings located in the outer layer and the magnetizing coils wound on the inner layer. The AlNiCo magnets are embedded between the two layers and can be protected from the unintentionally irreversible demagnetization.

In [39], a multimode design method is proposed for motor design under multiple operation conditions. In [41], a novel dual-mode operation is proposed: DSPM mode when PMs are normally magnetized and switched-reluctance (SR) mode when PMs are totally demagnetized. A new algorithm by combining Preisach theory and time-stepping FEM (TS-FEM) is developed to rapidly and accurately predict the electromagnetic performance of DS-VFMM [42]. A phase-transformed design of stator windings is also proposed to minimize the torque

ripple of DS-machines [43]. The suitability for integrated-starter-generator (ISG) and the optimization of the magnet proportions of DM-DSMM are analyzed in [44] and [45]. The "pole-changing" concept is introduced to a DS-VFMM [46], which can provide multiple operating modes to further extend the CPSR.

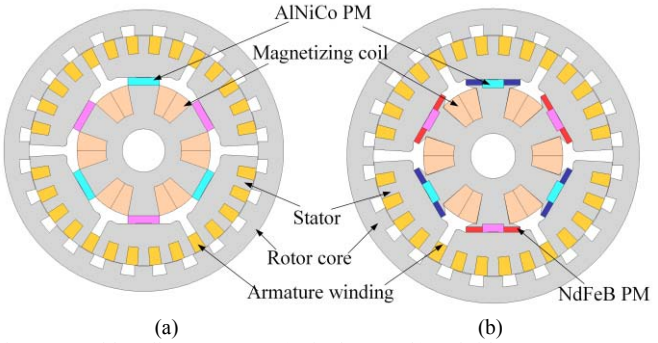

Fig. 14. Doubly salient VFMM. (a) Single-PM. (b) Hybrid-PM.

2) Switched Flux

The switched flux topologies [47]-[61] are applied to memory machines [8], i.e. so-called switched flux VFMM (SF-VFMM). The SF-VFMM combines the advantages of high torque density, by utilizing neodymium-iron-boron (NdFeB) magnets, and the excellent flux adjustability of LCF magnets [47]-[51]. Moreover, the bipolar and sinusoidal flux-linkage allows standard three-phase inverters and conventional vector control to be used to drive the machines. Thus, the torque quality can be improved compared to the DS counterparts [40].

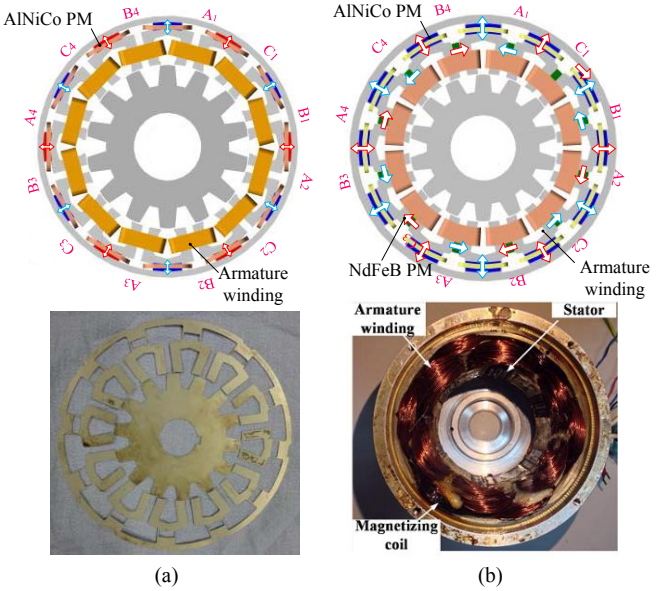

Fig. 16. Switched flux VFMM. (a) Single-PM. (b) Hybrid-PM.

Two novel SF-VFMMs with either single-PM or hybrid-PM topologies are presented as shown in Fig. 16. The design methodologies of the single-PM and hybrid-PM structures are given in [47] and [48], respectively. Based on the simplified magnetic circuit modeling, the analytical expressions of key electromagnetic parameters of the machines are derived [48]-[50]. It is found that the significant design conflicts exist on the stator, and it is necessary to realize a design trade-off between the wide MS range and the high torque capability during the design stage. In a similar way, two axial-field SF-VFMMs with parallel [55] and series [56] hybrid-PM arrangements are proposed to further improve the torque density compared to their radial-flux counterparts.

The "winding function switching (WFS)" concept for magnetizing windings is proposed. Based on this concept, "hybrid excitation (HE)" [57] and "DC-to-AC switching" [58] SF-VFMMs are proposed, respectively. The influence of "HE" operation on the electromagnetic characteristics of the proposed SF-VFMM is evaluated, and the feasibility of "DC-to-AC switching" is confirmed with the FW performance improvement.

In [59], the nonlinear mathematical model of the proposed SF-VFMM is built, and the simulation of the drive control system is conducted based on MATLAB/Simulink platform, as shown in Fig. 17. A stepwise magnetization control strategy for the machine is proposed according to the specific operating characteristics at different MSs. Besides, the effectiveness of the control strategy is experimentally validated, as reflected in the measured torque/power-speed curves in Fig. 18.

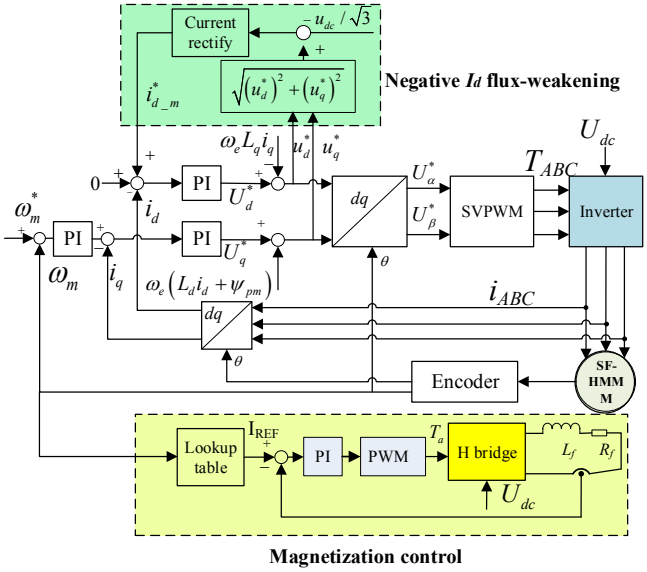

Fig. 17. Overall block diagram of the proposed global control strategy.

3) Flux Reversal

For the preceding mentioned DS- and SF-VFMMs, the segmented stator makes the manufacturability relatively complicated. Besides, the LCF PMs are inserted in the outer side of stator, which inevitably increases the peripheral dimension and hence reduces the torque density. Therefore, some novel flux-reversal VFMMs (FR-VFMMs) having single-PM [62][63] and hybrid-PM [64] configurations are developed by the authors as shown in Fig. 19 by combining VFMM concept and FR structures. The flux regulation principle of the FR-VFMMs is represented in Fig. 20 by the open-circuit field distributions and phase flux linkage waveforms under different MSs.

The proposed FR-VFMMs feature consequent pole (CP) hybrid magnets are mounted on the stator poles. The LCF PMs are located between the adjacent stator teeth. Different from the single-PM counterpart, the NdFeB magnets are placed in the

middle of stator tooth surface for the hybrid-PM FR-VFMM. The stator consequent-pole arrangement permits the further performance improvements: 1) less armature demagnetization risk since the PMs and armature fluxes are in parallel; 2) reduced effective air-gap length which is favorite to over-loading operation; 3) relatively simple stator and rotor fabrication similar to switched reluctance machines. Meanwhile, the hybrid magnet configuration allows flexible flux regulation without much sacrificing torque density.

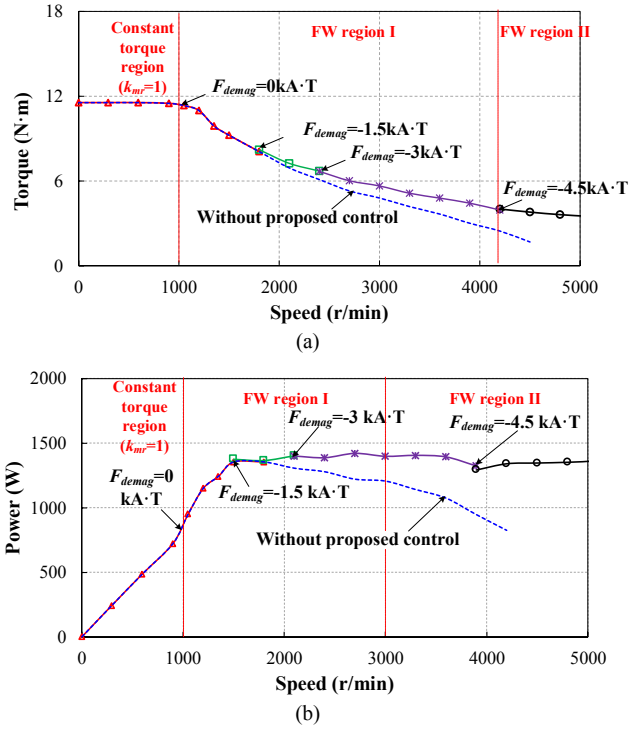

Fig. 18. Measured torque/power speed curves of the prototype hybrd-PM SF-VFMM with or without the proposed control strategy. (a) Torque-speed. (b) Power-speed.

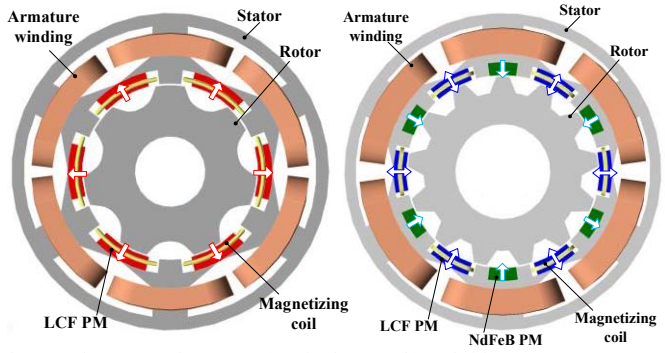

Fig. 19. Flux-reversal VFMM. (a) Single-PM. (b) Hybrid-PM.

Furthermore, the variable-mode operation is implemented on a single-PM FR-VFMM [62], and the corresponding variable-mode circuit diagram is presented in Fig. 21. Similar to "pole-changing" concept, the magnetic pole number can be varied to fulfil the torque and speed requirements over a wide operating range. The machine with all magnetized PM poles can offer high torque output, while that with half magnetized PM poles can provide wide constant power range. In addition, the FR-VFMM with non-magnetized PMs can be considered as a dual-three phase electrically excited reluctance machine, which can be fed by an open-winding based dual inverters to provide the direct current (DC) bias excitation to further extend the speed range.

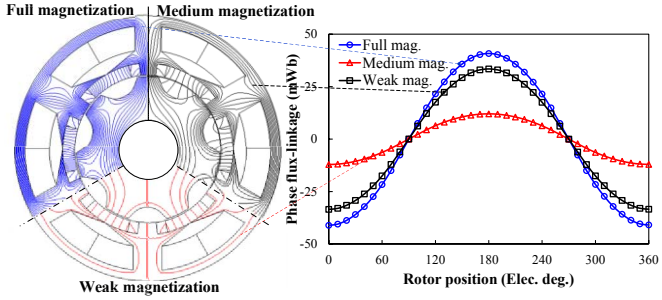

Fig. 20. Flux regulation principle of proposed FR-VFMM. (a) Open-circuit field distribution. (b) Open-circuit flux-linkages (400r/min).

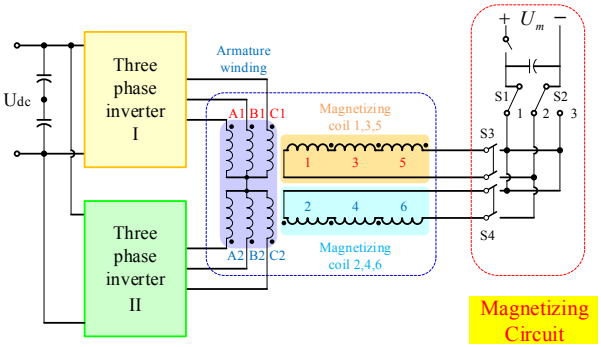

Fig. 21. Variable-mode circuit diagram for the proposed FR-VFMM.

4) Variable Reluctance

Fig. 22 shows the typical structure of the variable reluctance VFMM (VR-VFMM) proposed by the authors [65], which is geometrically characterized by a doubly salient structure having hybrid magnets mounted on the stator poles. The variable-flux AlNiCo PMs are placed in the middle of the stator pole, while the sided constant-flux NdFeB PMs serve as a major flux contributor for the air-gap flux. Furthermore, the DC magnetizing coils are wound on the stator teeth having PMs. The MS of AlNiCo magnets can be flexibly adjusted via a current pulse fed by the magnetizing coils. Those stator teeth without PMs carry single-layer non-overlapping armature windings. As a result, the consequent pole arrangement allows the LCF PMs to effectively resist the demagnetization risk caused by the armature reaction.

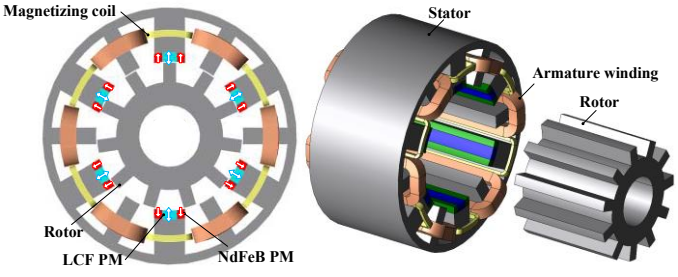

Fig. 22. Topology of the proposed 12/11-pole VR-HMMM. (a) Cross-section. (b) Exploded view.

The steady-state torque and torque versus current density curves of the VR-VFMMs with different rotor poles are compared in Fig. 23. It shows that the even- rotor-pole machines exhibit much higher torque ripples than the odd-rotor-pole counterparts. Moreover, the 10-pole machine exhibits the highest torque capability under the rated load operation, followed by the 11-rotor one, while the lowest over-loading capability can be observed in the 13-pole one.

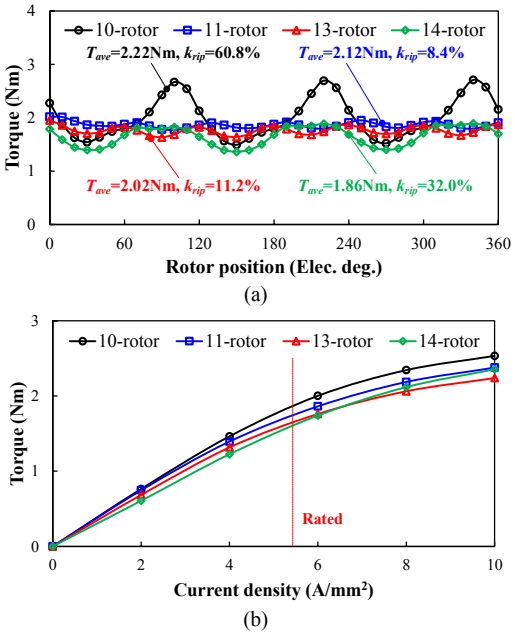

Fig. 23. Comparison of torque characteristics. (a) Steady-state torque waveforms, I_d=0 control, rated current density=5.5A/mm^2. (b) Torque against current density curves.

B. *Rotor-PM Type*

1) Claw Pole

A claw-pole VFMM is proposed in [66], where the AlNiCo PM ring and the magnetizing coils are embraced by the left and right claw poles. The PM ring is axially magnetized, and its magnetic flux can circulate through the claw poles and enter the air-gap to couple with the armature windings. Moreover, the magnetizing coils are wound around the PM ring. Hence, the MS of AlNiCo PM can be conveniently varied by injecting a DC current pulse into the magnetizing coil. The claw-pole structure can well facilitate the modular manufacturing and mass production, which is suitable for the automotive industry. However, the significant flux leakage, low torque density and low power factor are the major concerns.

2) Radial/Axial Flux

A mixed radial/axial field VFMM [66] is developed as shown in Fig. 24 by sandwiching variable flux material-AlNiCo between two twistable surface-mounted PM machines having NdFeB magnets [67]. The DC-magnetizing coils are embedded on stator. However, this machine is extremely complicated for manufacturing. The long flux path and low axial permeability result in bulky DC-magnetized coils.

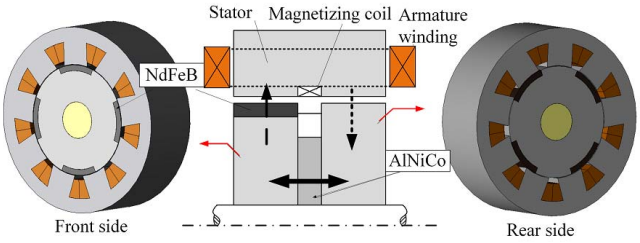

Fig. 24. Radial/axial mixed field VFMM configuration.

V. Newly Developed VFMMs for Performance Improvement

A. *Major Merits and Demerits of Existing VFMMs*

1) AC-magnetized

Overall, for the AC-magnetized VFMMs, the flux varying and electromagnetic energy conversion functions are integrated in the armature winding, which eliminates the additional circuit and converters compared to their DC-magnetized counterparts. Specifically, the parallel magnetic circuit type is reported as more advantageous in terms of the inverter cost saving, because smaller current pulses are able to change the MSs of the LCF magnet since it is not directly supported with the flux from the high coercive force (HCF) magnet. However, the HCF magnet may be beneficial to support the LCF magnet under load current and avoid undesired demagnetization.

2) DC-magnetized

Generally, the DC-magnetized VFMMs can conveniently perform online magnetization with the aid of the DC magnetizing coils. For the stator-PM structures, the highly robust structure and mechanical reliability are obtained. In addition, compared to DS-VFMMs having high torque ripple and low torque density, SF-VFMMs exhibit sinusoidal symmetrical phase back-EMFs and lower torque ripples and higher torque densities. Nonetheless, the torque is dominated by the PM torque instead of the reluctance torque. Hence, the torque density is lower than that of IPM-VFMM which can provide additional reluctance torque. Furthermore, the crowded and relatively complicated stator can be observed in DS- and SF-VFMMs, resulting in their limited torque density. The alternative topologies having simpler stator and easier manufacturing are presented, e.g., FR and VR structures, but their design methodologies and complete optimizations still remains unresolved.

The rotor-PM DC-magnetized VFMMs with radial/axial mixed fields are relatively mechanically complicated and require expensive soft magnetic composite (SMC) to allow three-dimensional (3D) magnetic path, which is currently unfavorable for industrial applications.

In order to alleviate the aforementioned problems, some improved VFMM designs are further developed, and the derivation of the novel designs for performance improvements is shown in Fig. 25.

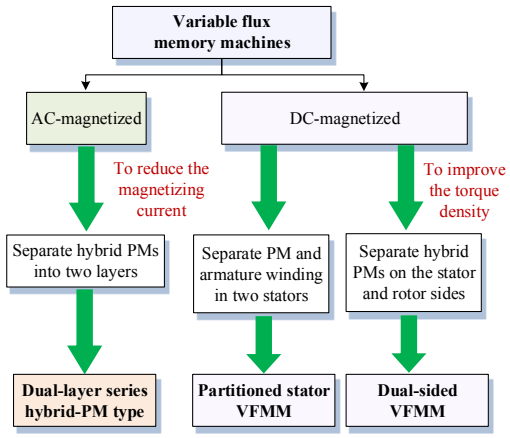

Fig. 25. The derivation of design improvement for the existing VFMMs.

B. *Improved AC-magnetized Topology*

A novel dual-layer PM VFMM (DLPM-VFMM) is proposed in [69] by the authors in order to address the aforementioned issues. As shown in Fig. 26, compared to the conventional series VF-HMM, two sets of magnets are separated within one PM pole. The NdFeB PMs are located close to the air-gap, which serve as a main flux contributor for torque production. Besides, the LCF PMs are placed in the inner space close to the shaft side, which act as an air-gap flux adjustor. The DLPM arrangement permits the following performance improvements: 1) The hybrid magnet configuration allows flexible flux regulation without much sacrificing torque density; 2) The on-load armature demagnetization risk is eliminated since the LCF PMs and NdFeB PM fluxes are magnetically in series; 3) A bypass branch is designed for the *d*-axis magnetizing MMF. This is helpful to the effective reduction of the current pulse level and inverter rating.

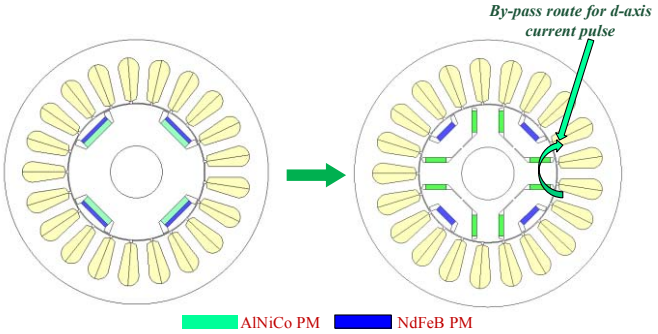

Fig. 26. Topologies of the existing and proposed series hybrid-PM VFMMs. (a) Conventional (single-layer PM, SLPM). (b) DLPM.

C. *DC-magnetized Topologies*

1) Partitioned Stator

a) Variable Flux Type

The proposed 6-stator-slot/11-rotor-pole partitioned stator VFMMs (PS-VFMMs) having different PM types are proposed by the authors as shown in Fig. 27 [69]-[74]. The non-overlapping tooth-coil windings are employed in the outer stator, whilst the separate rotor iron poles are sandwiched between two stators. In addition, the PM excitations in the original single-stator structures having either flux reversal (FR) or switched flux (SF) topologies are moved to a secondary inner stator. Meanwhile, the inner stator can be generally designed as three PM types, i.e., so-called surface-mounted PM (SPM), U-shaped IPM (UIPM), and spoke-type IPM (SIPM) as shown in Figs. 27(a), (b), and (c), respectively.

Fig. 28 shows the flux regulation principle represented by the flux line plots at flux-enhanced and flux-weakened states, respectively. It can be seen that the air-gap flux can be either enhanced or weakened when the LCF PMs are magnetized identically or oppositely with the NdFeB PMs.

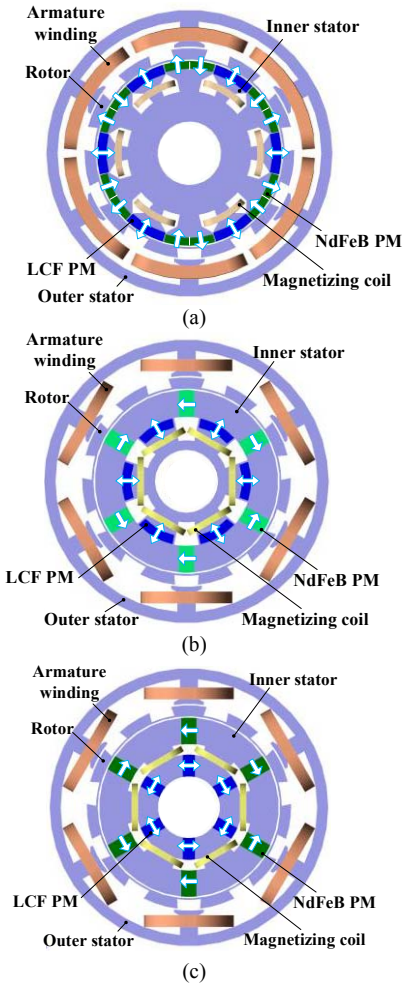

Fig. 27. Topologies of the proposed PSMMs. (a) SPM. (b) UIPM. (c) SIPM.

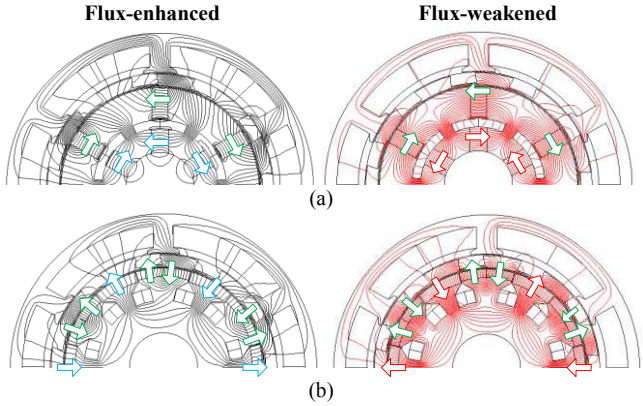

Fig. 28. Flux regulation principle. (a) SIPM. (b) SPM.

Moreover, the fundamental back-EMFs of the two machines at 400r/min as functions of the magnetization ratio of LCF PMs are plotted in Fig. 28(a). It can be observed that the SIPM

machine shows the widest flux regulation range due to heavier magnetic saturation in the inner stator for the SPM structure. In addition, the SPM machine has the lowest flux regulation capability owing to the large air-gap magnetic reluctance for the short-circuiting PM fluxes. Fig. 28(b) shows the torque versus current curves. The SPM machine exhibits lower torque under rated load, but higher over-loading capability. This is mainly attributed to the greater PM flux leakage in the SPM machine, which leads to less magnetic saturation in the outer stator.

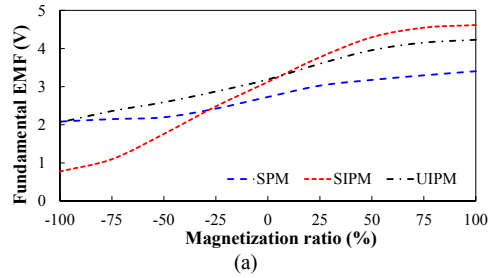

(a)

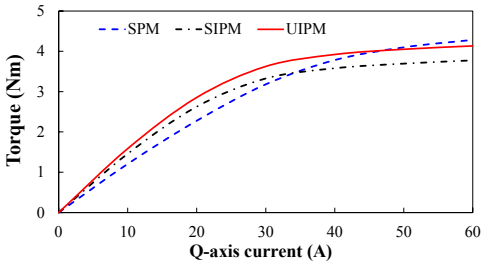

(b)

Fig. 29. Comparison of electromagnetic performance of various PSMMs. (a) Variation of back-EMF fundamental magnitude with the magnetization ratio of LCF PMs. (b) Torque versus *q*-axis current curves.

b) Pole-Changing Type

The "pole-changing" concept [33] is applied to PS-VFMM with spoke-type LCF PMs [74]. The magnetization level and polarity of the LCF PM can be purposely changed. Thus, the inner stator PM arrangement can be regrouped into either 12- or 6-pole mode. Subsequently, this new machine can behave similarly as the conventional 12-pole and 6-pole E-core switched flux PM machines, respectively. The configuration of the proposed variable mode PS-VFMM is shown in Fig. 29. The armature windings and PM excitations are separately placed in the dual stators. The flux-concentrated spoke-type LCF PMs are embedded in the inner stator, and the toroidal magnetizing windings are located in the slots adjacent to the PM ends. The magnetizing windings serve as PM polarity adjustors which enable the machine to operate at the different modes. The illustration of three modes and the corresponding field distributions are shown in Figs. 30~32, respectively.

The torque-speed curves corresponding to the different modes can be calculated as shown in Fig. 33. According to the intersection points of torque-speed curves at different modes, the whole operation speed range can be classified into three regions: low-speed region I (0~ω_1), medium-speed region II (ω_1~ω_2), and high-speed region III (ω_2~ω_3). ω_1 and ω_2 are the corresponding critical speeds for torque-speed curves of mode-I and II, and ω_3 is the maximum speed point when machine operates within region III. Evidently, the effective speed range extension can be realized via the PM pole-changing actions, which simplifies the control effort.

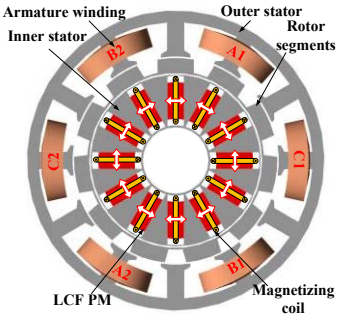

Fig. 29. Topology of 12/11-pole variable mode PSMM.

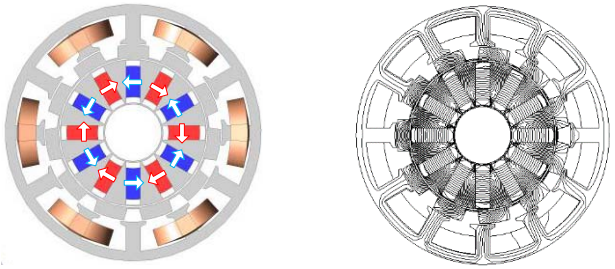

(a) (b)

Fig. 30. Cross-section view and field distribution of PS-SFMM at mode-I. (a) Configuration. (b) Field distribution.

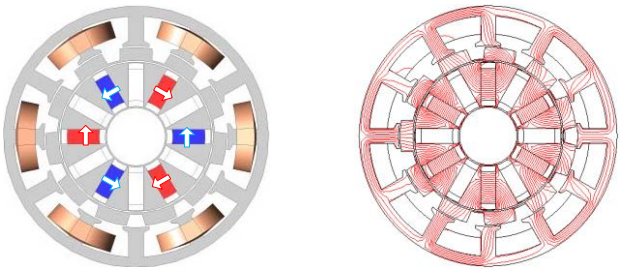

(a) (b)

Fig. 31. Cross-section view and field distribution of PS-SFMM at mode-II. (a) Configuration. (b) Field distribution.

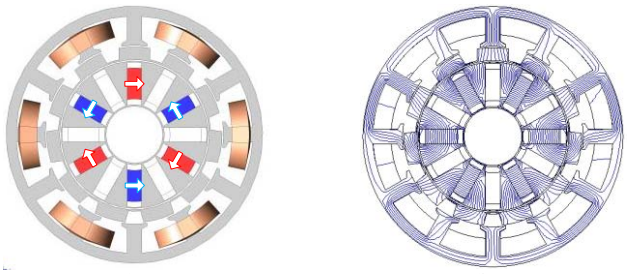

(a) (b)

Fig. 32. Cross-section view and field distribution of PS-SFMM at mode-III. (a) Configuration. (b) Field distribution.

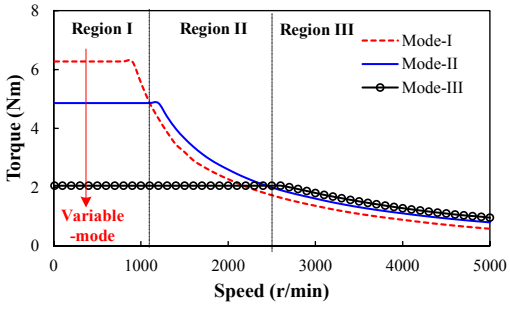

(a)

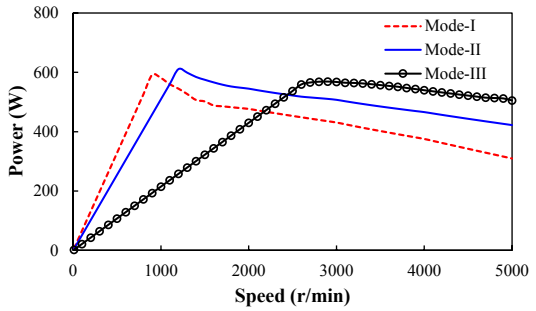

(b)

Fig. 33. FE-predicted torque/power-speed characteristics of variable mode PSMM at different modes, DC-link voltage=60V, maximum phase current=20A. (a) Torque-speed curve. (b) Power-speed curve.

2) Dual-Sided PM

A novel dual-sided PM VFMM (DSPM-VFMM) [75] is proposed by combining the distinct advantages of "high torque density" of conventional rotor-PM machine and "simple online PM flux control" of stator-PM VFMM. The proposed topology and operating principle are shown in Figs. 34 and 35, respectively. The consequent-pole NdFeB PMs are placed in the rotor, while the LCF PMs are mounted between the adjacent stator teeth to enable flexible air-gap flux adjustment.

The major advantages of the developed machine, which combines the distinct synergies of the conventional rare-earth PM machine and stator-PM MM, which can be summarized as follows:

1) The merits of high torque density of conventional rotor-PM machine and the easy magnetization control of stator-PM MM can be well synthesized;

2) The wide speed range and the high efficiency at CPSR can be realized due to excellent flux adjusting capability and negligible excitation copper loss in the proposed DSPM-MM.

3) The parallel PMs and armature reaction fields can prevent the LCF PMs from accidental armature demagnetization.

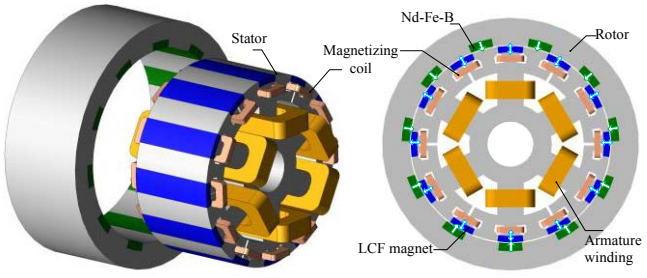

(a) (b)

Fig. 34. Proposed DSPM-VFMM. (a) Exploded view. (b) Cross-section.

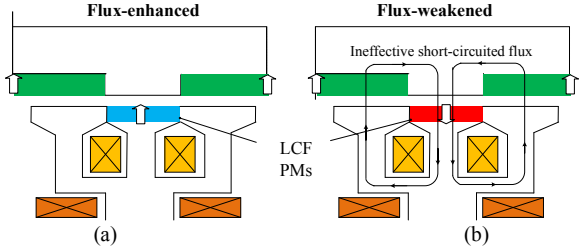

(a) (b)

Fig. 35. Field regulation principle. (a) Flux-enhanced. (b) Flux-weakened.

VI. Comparison of SFMM and Various Conventional Machines for Traction Applications

The SF-VFMM with upscaling power rating is taken as an example to confirm the merit of VFMM in the context of potential traction applications. The cross-section view of the SF-VFMM with 12-stator slot/14-rotor tooth structure is shown in Fig. 36. The basic design parameters of the SF-VFMM are listed in Table I.

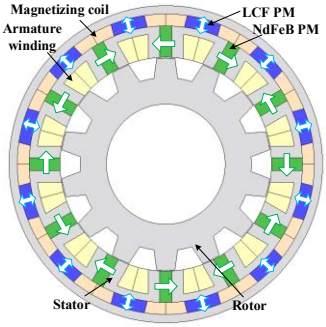

Fig. 36. Cross-section of the 12-stator slot/14-rotor tooth SF-VFMM.

TABLE I
MAIN SPECIFICATIONS OF THE 12-STATOR SLOT/14-ROTOR TOOTH SF-HPMMM AND 12 SLOT/10 POLE SPM/IPM MACHINES

Items	Parameters
DC-link voltage (V)	650
Stator outer diameter (mm)	264
Stator inner diameter (mm)	198
Air-gap length (mm)	0.73
Active stack length (mm)	50.8
Rotor pole bottom width (mm)	18.1
Rated current (Arms)	252
Turns of winding per phase	64
NdFeB magnet thickness (mm)	10.3
NdFeB magnet width (mm)	21.5
NdFeB magnet grade	N35SH
LCF magnet thickness (mm)	12.2
LCF magnet width (deg)	12
LCF magnet grade	SB12B
Stator phase resistance @20°C (Ω)	0.038
Steel material	35CS440

The key electromagnetic characteristics of the SF-VFMM are compared with those of the conventional machines, including IM, synchronous reluctance machine (SynRM), PM-assisted SynRM, and Prius 2010 IPM machine [76][77], The four conventional machine topologies are shown in Fig. 37. The corresponding key specifications of the four machines are listed in Table II. It should be note that in order to perform the comparison fairly, these machines for comparison are designed with identical outer diameter, stack length, packing factor, air-gap length, rated current density of 26.4 A/mm^2, and rated DC-link voltage of 650V.

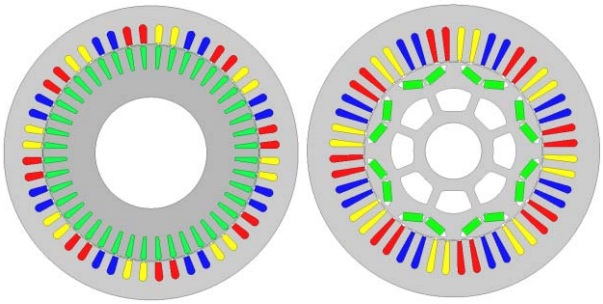

(a) (b)

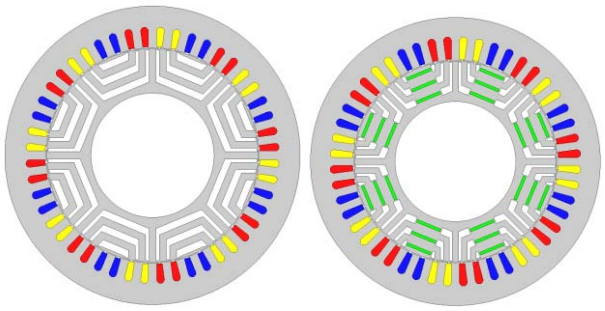

(c) (d)

Fig. 37. Cross-sections of the AC sychoronous machine topologies for tractrion applications. (a) 48-stator slot/44-rotor slot/8-pole Induciton machine. (b) 48-slot/8-pole Prius 2010 IPM machine. (c) 48-slot/8-pole SynRM. (d) 48-slot/8-pole PM-assisted SynRM.

TABLE II
KEY SPECIFICATIONS OF FOUR INVESTIGATED CONVENTIONAL MACHINES

Machine types	IM	IPM	SynRM	PM-assisted SynRM
DC-link voltage	650			
Stator slot number	48			
Rotor pole number	8			
Rotor slot number	44	-		
Stator outer diameter (mm)	264			
Stator inner diameter (mm)	195	161.9	199	182.4
Number of barriers	-	1	4	
Active length (mm)	50.8			
Air-gap length (mm)	0.73			
Packing factor	0.465			
Rated current density (A/mm^2)	24.6			
Number of turns per phase	56	88	56	80
Stator slot height (mm)	13.85	30.9	12.2	22.53
Stator opening width (mm)	8.77	7.55	8.18	7.55
Stator phase resistance @20°C (Ω)	0.080		0.077	
Number of parallel branches	1			
Steel grade	35CS440			
Magnet grade	-	N35SH	-	N35SH

In order to confirm the overall efficiency improvement of the SF-VFMM over a wide operating range, its efficiency map with abovementioned optimal torque-speed envelop is plotted in Fig. 38. While the efficiency maps of the four conventional machines are shown in Fig. 39. It can be observed that the proposed machine exhibits a larger high-efficiency area (>90%), particularly at low-speed cases, compared to the four conventional machines. This is mainly attributed to the short end windings and reduced copper loss, which is a dominant loss component at low speeds. Meanwhile, it can be seen that the high efficiency can be maintained over a wide operating range by combining the highest efficiency characteristics under different magnetization states. For instance, the positive magnetizing operation is preferred for constant-torque operation to obtain high efficiency, whereas the negative magnetization states are beneficial for CPSR with the minimized iron losses, which is identified as the dominant loss component at high-speed region. The aforementioned investigation confirms that the advantage of the proposed global FW control strategy for the SF-VFMM in terms of the efficiency improvement over a wide operation range.

On the other hand, the maximum operating region (92.23%) covering high efficiency region more than 92% can be observed in the SF-VFMM, which is mainly attributed to the forgoing developed expendable-speed control scheme. The maximum efficiency of the SynRM is much lower than IPM due to its low torque capability, while the efficiency map of the PM-assisted SynRM is close to that of the IPM. In addition, the overall efficiency of the IM is lower than those conventional PM counterparts. For example, the maximum efficiency of the IM with copper squirrel cage (94.2%) is ~2% lower than that of the SF-VFMM (96.3%), due to the low torque capability under low electric loading and rotor copper loss.

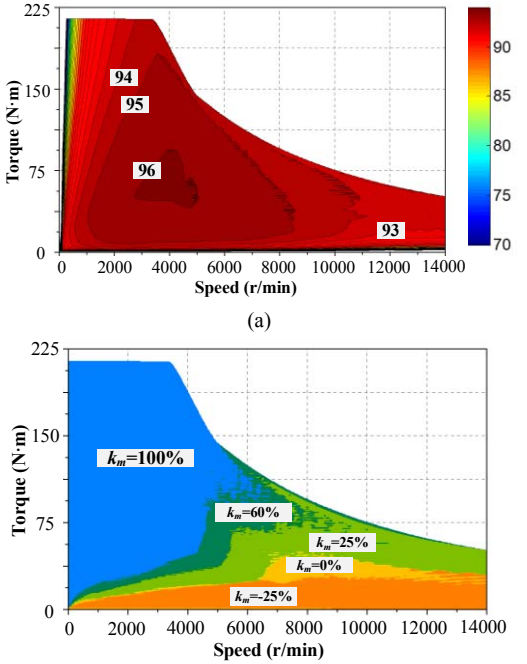

(a)

(b)

Fig. 38. Overall efficiency map of the proposed SF-VFMM by combining highest efficiency at different MSs. (a). Resultant efficiency map. (b) Optimal magnetization state distribution.

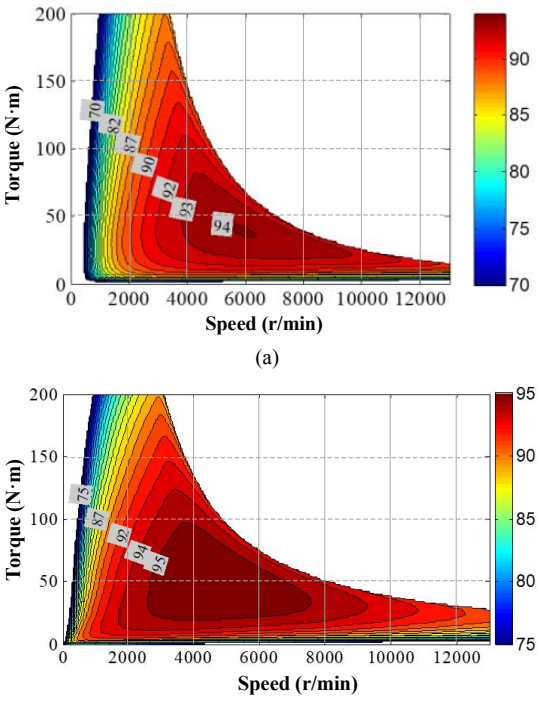

(a)

(b)

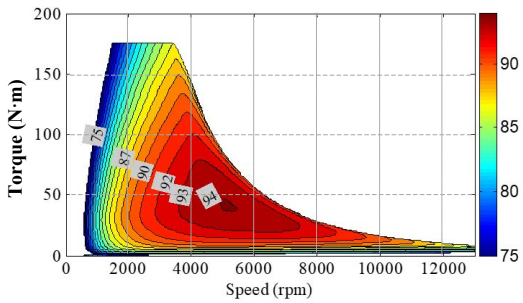

(c)

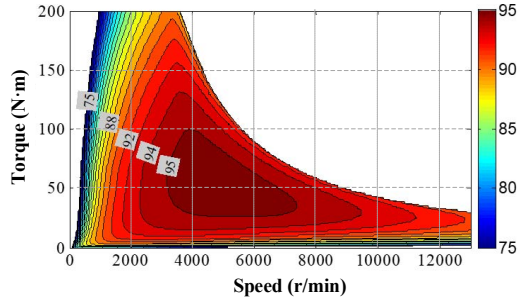

(d)

Fig. 39. Efficiency maps of conventional machines. (a) Induction machine. (b) Prius 2010 IPM machine. (c) SynRM. (d) PM-assisted SynRM.

The torque/power-speed curves of the proposed SF-VFMM and the four conventional machines are compared in Fig. 40. It can be seen that the SynRM has the lowest torque density and the limited CPSR. The PM-assisted SynRM and the SF-VFMM have comparable torque capability with the IPM machine, while the SF-VFMM exhibits best FW capability with widest CPSR. The IM shows slightly higher maximum torque than the IPM machine at the maximum current due to that the former has better overload capability. However, the IM still suffers from a restricted CPSR than its PM counterparts.

The weight, material cost and related torque density of the investigated machines are listed in Table III. The PM-assisted SynRM uses 30% less NdFeB PM than the IPM machine. The material cost of SynRM is the cheapest, about ~1/3 of IPM. The PM-assisted SynRM and the IM are 25% and 50% cheaper than the IPM respectively. The material cost of SF-VFMM is slightly higher than that of the IPM machine. Thus, the SynRM and the IM have great advantage over the SF-VFMM and the IPM in terms of material cost. However, the PM-assisted and the SF-VFMM have higher torque density than other machines. Considering the advantages of the overall efficiency improvement, excellent FW capability and acceptable torque density, the SF-VFMM is a potentially attractive candidate for traction applications.

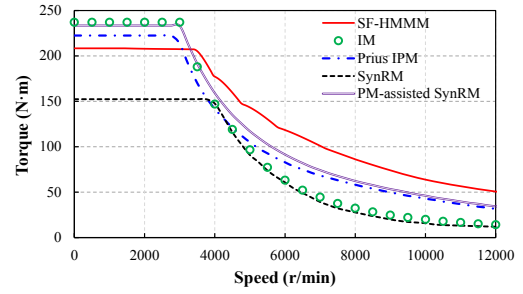

(a)

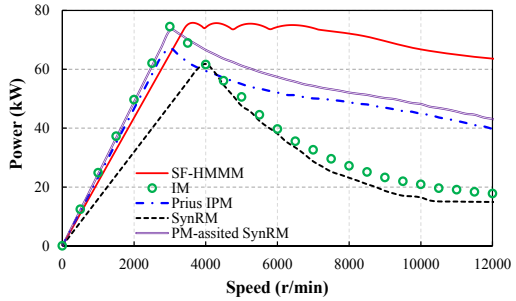

(b)

Fig. 40. Torque/power-speed maps of the proposed SF-VFMM under the proposed global FW control strategy. (a). Torque-speed. (b) Power-speed.

TABLE III
COMPARISON OF MATERIAL COST AND TORQUE DENSITY IN THE INVESTIGATED MACHINES

Machine types	SF-VFMM	IM	IPM	SynRM/PM-assisted SynRM
Stator copper mass(kg)	2.98	3.36	4.93	4.1/4.1
Iron mass (kg)	13.7	15.0	15.1	12.8/12.4
Rotor copper/NdFeB mass (kg)	0.62	3.92	0.77	-/0.545
LCF mass (kg)	0.46	-	-	-
Total mass (kg)	17.8	22.2	20.75	16.1/18.1
Torque/total mass (Nm/kg)	11.74	10.68	10.69	9.44/12.87
Stator copper price (£)	11.6	17.5	34.51	14.21/28.7
Iron (£)	22.3	29.9	30.08	25.7/24.9
NdFeB PM (£)	62.4	-	77.5	-/54.5
LCF PM (£)	55.3	-	-	-
Rotor copper (£)	-	28.5	-	-
Total (£)	151.6	80.9	142.1	41.66/110

VII. CONCLUSIONS AND DISCUSSIONS: MAJOR CHALLENGES AND DEVELOPMENT TRENDS

This paper reviews the recent developments of VFMMs with particular reference to the newly emerged machine topologies and the related control strategies. The major merits and demerits of various VFMM topologies are identified and summarized. In order to alleviate the major drawbacks in the existing structures, some novel VFMM designs are proposed. It is found that the developed VFMMs can effectively reduce the magnetizing current level and further improve the torque density compared to its conventional counterpart. The electromagnetic characteristics of an EV scaled SFMM are compared with those of the conventional traction machine candidates. It shows that the SFMM exhibits the advantages of efficiency improvement over wider speeds and loads, excellent FW capability, as well as acceptable torque density

Following the overview on recent VFMM technologies, some general comments are presented regarding the current challenges and development trends, which can be summarized as follows:

A. Current Challenges:

1) There are two important constraints regarding the magnetizing current of VFMMs. First, the positive *d*-axis current required to fully magnetize, i.e., increase MS to 100%, must be small enough to make it be within the inverter capability. Secondly, the heaviest load condition (i.e., maximum torque) must not force the magnet

operating point below the knee of the *B-H* curve to avoid the unintentional demagnetization. In this case, the maximum torque capability will be reduced;

2) The exploration of advanced VFMM topologies to effectively improve the torque density is still a challenging issue. The AC-magnetized structure seems to be more suitable for traction applications due to its higher torque density than its DC-magnetized counterparts and has no need for another independent magnetization control circuit;
3) A workable and practical numerical hysteresis model for the LCF magnet material with more linear magnetizing characteristics is required to facilitate the design process as well as generating a workable look-up table for aiding the test stage;
4) A more accurate PM flux linkage observation is essential for dynamic performance improvement of the whole drive system. Besides, an effective approach to the transient pulsating torque mitigation is still a major challenge for the application of VFMM in the future EV drive system;
5) A coordinated scheme for drive/magnetization control is still unreported particularly for AC-magnetized VFMM.
6) More significantly simplified VFMM topologies are still highly desirable.

B. Future Trends:

1) Novel VFMM topologies will continue to emerge, which attempt to improve the torque density, prevent the unintentional demagnetization, and reduce the magnetizing current level;
2) The integration of the available hysteresis model into commercial FE software will facilitate the rapid computation and design optimization process for VFMMs;
3) The inherent relationship between various design parameters needs to be better identified and quantified, which is helpful for the multi-objective design of various VFMMs;
4) The global FW control strategy accounting for both speed range extension and efficiency improvement is required for the VFMMs applicable for EV applications;
5) The application aspects of VFMMs to traction applications need to be investigated in depth, which mainly include the advanced PM flux linkage estimation technique, electromagnetic-thermal coupling analysis, vibration and structural dynamics, as well as high-speed fault tolerance control scheme.

REFERENCES

[1] Z. Q. Zhu and D. Howe, "Electrical machines and drives for electric, hybrid, and fuel cell vehicles," *Proc. IEEE*, vol. 95, no. 4, pp. 746-765, Apr.2007.

[2] Z. Q. Zhu, "Permanent magnet machines for traction applications," in *Encyclopaedia of Automotive Engineering,* John Wiley & Sons, Ltd., 2014.

[3] A. M. EL-Refaie, "Motors/generators for traction/propulsion applications: a review," *IEEE Veh. Technol. Mag*., vol. 8, no. 1, pp. 90-99, Mar. 2013.

[4] I. Boldea, L. N. Tutelea, L. Parsa, and D. Dorrell, "Automotive electric propulsion systems with reduced or no permanent magnets: an overview," *IEEE Trans. Ind. Electron*., vol. 61, no. 10, pp. 5696-5711, Oct.2014.

[5] I. Boldea, "Electric generators and motors: an overview," *CES Trans. Electr. Machin. and Syst*. vol. 1, no. 1, pp. 3-14, Mar. 2017.

[6] K. T. Chau, C. C. Chan, and C. Liu, "Overview of permanent-magnet brushless drives for electric and hybrid electric vehicles," *IEEE Trans. Ind. Electron*., vol. 55, no. 6, pp. 2246-2257, May 2008.

[7] M. Tursini, E. Chiricozzi, and R. Petrella, "Feedforward flux-weakening control of surface-mounted permanent-magnet synchronous motors accounting for resistive voltage drop," *IEEE Trans. Ind. Electron*., vol. 57, no. 1, pp. 440-448, Jan. 2010.

[8] V. Ostovic, "Memory motors," *IEEE Ind. Appl.* Mag., vol. 9, no. 1, pp. 52-61, Jan./Feb. 2003.

[9] H. Liu, H. Lin, S. Fang, and Z. Q. Zhu, "Permanent magnet demagnetization physics of a variable flux memory motor," *IEEE Trans. Magn.*, vol. 45, no. 10, pp. 4736-4739, Oct. 2009.

[10] H. Yang, H. Lin, Z. Q. Zhu, and S. Lyu, "Influence of magnet eddy current on magnetization characteristics of variable flux memory machine," *AIP Advances*, vol. 8, no. 5, Article No. 056602, 2018.

[11] N. Limsuwan, T. Kato, K. Akatsu, and R. Lorenz, "Design and evaluation of a variable-flux flux-intensifying interior permanent magnet machine," *IEEE Trans. Ind. Appl.*, vol. 50, no. 2, pp. 1015-1024, Mar./Apr. 2014.

[12] C. Yu, T. Fukushige, N. Limsuwan, T. Kato, D. Diaz Reigosa, and R. D. Lorenz, "Variable-flux machine torque estimation and pulsating torque mitigation during magnetization state manipulation," *IEEE Trans. Ind. Appl.*, vol. 50, no. 5, pp. 3414-3422, Feb. 2015.

[13] B. S. Gagas, K. Sasaki, T. Fukushige, A. Athavale, T. Kato, and R. D. Lorenz, "Analysis of magnetizing trajectories for variable flux pm synchronous machines considering voltage, high-speed capability, torque ripple, and time duration," *IEEE Trans. Ind. Appl.*, vol. 52, no. 5, pp. 4029-4038, Jun. 2016.

[14] T. Fukushige, N. Limsuwan, T. Kato, K. Akatsu, and R. D. Lorenz, "Efficiency contours and loss minimization over a driving cycle of a variable flux-intensifying machine," *IEEE Trans. Ind. Appl.*, vol. 51, no. 4, pp. 2984-2989, Jul./Aug. 2015.

[15] T. Fukushige, N. Limsuwan, T. Kato, K. Akatsu, and R. D. Lorenz, "Efficiency contours and loss minimization over a driving cycle of a variable flux-intensifying machine," *IEEE Trans. Ind. Appl.*, vol. 51, no. 4, pp. 2984-2989, Jul./Aug. 2015.

[16] B. S. Gagas, K. Sasaki, A. Athavale, T. Kato, and R. Lorenz, "Magnet temperature effects on the useful properties of variable flux PM synchronous machines and a mitigating method for magnetization changes," *IEEE Trans. Ind. Appl.*, vol. 53, no. 3, pp. 2189-2199, May/Jun. 2017.

[17] S. Maekawa, K. Yuki, M. Matsushita, I. Nitta, Y. Hasegawa, T. Shiga, T. Hosoito, K. Nagai, and H. Kubota, "Study of the magnetization method suitable for fractional-slot concentrated-winding variable magnetomotive-force memory motor," *IEEE Trans. Power Electron.*, vol. 29, no. 9, pp. 4877-4887, Sep. 2014.

[18] K. Sakai, K. Yuki, Y. Hashiba, N. Takahashi, and K. Yasui, "Principle of the variable-magnetic-force memory motor," in *Proc. Int. Conf. Electr. Mach. Syst.*, Tokyo, Japan, 2009, pp. 1-6.

[19] Y. Nariaki, and K. Sakai, "A permanent magnet motor capable of pole changing for variable speed drive," in *Proc. Int. Conf. Elect. Mach. Syst. (ICEMS)*, Busan, 2013, pp. 1127-1132.

[20] A. Sun, J. Li, R. Qu, J. Chen, and H. Lu, "Rotor design considerations for a variable-flux flux-intensifying interior permanent magnet machine with improved torque quality and reduced magnetization current," in *Proc. IEEE Energy Convers. Congr. Expo.*, Sep. 2015, pp. 784-790.

[21] J. Chen, J. Li, and R. Qu, "Maximum-torque-per-ampere and magnetization-state control of a variable-flux permanent magnet machine," *IEEE Trans. Ind. Electron.*, vol. 65, no. 2, pp. 1158-1169, Feb. 2018.

[22] M. Ibrahim, L. Masisi, and P. Pillay, "Design of variable-flux permanent magnet machines using Alnico magnets," *IEEE Trans. Ind. Appl.*, vol. 51, no. 6, pp. 4482–4491, Nov./Dec. 2015.

[23] M. Ibrahim, L. Masisi, and P. Pillay, "Design of variable flux permanent magnet machine for reduced inverter rating," *IEEE Trans. Ind. Appl.*, vol. 51, no. 5, pp. 3666–3674, Sep./Oct. 2015.

[24] A. M. Akrem and P. Pillay, "Novel flux linkage estimation algorithm for a variable flux PMSM," *IEEE Trans. Ind. Appl.*, 2018, in press.

[25] D. Wu, Z. Q. Zhu, A. Pride, R. Deodhar, and T. Sasaki, "Cross coupling effect in hybrid magnet memory machine" in *Proc. 7th IET Int. Conf. Power Electron. Machin. Drives, (PEMD),* Manchester, UK. 2014.

[26] Y. Zhou, Y. Chen, and J. X. Shen, "Analysis and improvement of a hybrid

permanent magnet memory motor," *IEEE Trans. Energy Convers.*, vol. 31, no. 3, pp. 915–923, Sep. 2016.

[27] A. Athavale, K. Sasaki, B. S. Gagas, T. Kato, and R. Lorenz, "Variable flux permanent magnet synchronous machine (VF-PMSM) design methodologies to meet electric vehicle traction requirements with reduced losses," *IEEE Trans. Ind. Appl.,* vol. 53, no. 5, pp. 4318–4326, Sep./Oct. 2017.

[28] A. Athavale, D. J. Erato, and R. Lorenz, "Enabling driving cycle loss reduction in variable flux PMSMs via closed-loop magnetization state control," *IEEE Trans. Ind. Appl*., 2018, in press.

[29] A. Athavale, K. Sasaki, T. Kato, and R. Lorenz, "Magnetization state estimation in variable-flux PMSMs," in *Proc. Int. Electr. Mach. Drives Conf. (IEMDC)*, Miami, FL, 2017, pp. 1-8.

[30] H. Hua, Z. Q. Zhu, A. Pride, R. P. Deodhar, and T. Sasaki, "A novel variable flux memory machine with series hybrid magnets," *IEEE Trans. Ind. Appl*., vol. 53, no. 5, pp. 4396-4405, Sept./Oct. 2017.

[31] Z. Q. Zhu, H. Hua, A. Pride, R. Deodhar, and T. Sasaki, "Analysis and reduction of unipolar leakage flux in series hybrid permanent-magnet variable flux memory machines," *IEEE Trans. Magn.*, vol. 53, no. 11, Art. No: 2500604, Nov. 2017.

[32] H. Hua, Z. Q. Zhu, A. Pride, R. P. Deodhar, and T. Sasaki, "Comparative study of variable flux memory machines with parallel and series hybrid magnets," in *Proc. Energy Convers. Congr. and Expo. (ECCE), 2017 IEEE*, Cincinnati, U.S., 2017, pp. 1-8.

[33] V. Ostovic, "Pole-changing permanent-magnet machines," *IEEE Trans. Ind. Appl.*, vol. 38, no. 6, pp. 1493-1499, Nov./Dec. 2002.

[34] K. Sakai, N. Yuzawa, and H. Hashimoto, "Permanent magnet motors capable of pole changing and three-torque-production mode using magnetization," *IEEJ J. Ind. Appl.*, vol. 2, no. 6, pp. 269–275, Jun. 2013.

[35] D. Wang, H. Lin, H. Yang, Y. Zhang, and X. Lu, "Design and analysis of a variable-flux pole-changing permanent magnet memory machine," *IEEE Trans. Magn.* vol. 51, no. 11, Art. No: 8113004, Nov. 2015.

[36] D. Wang, H. Lin, H. Yang, S. Fang, and Y. Huang, "Research on variable flux permanent magnet pole-changing machine with harmonic excitation," in *Proc. Int. Conf. Electr. Mach. Syst. (ICEMS)*, Hangzhou, China, 2014, pp. 1696-1700.

[37] D. Wang, H. Lin, H. Yang, Y. Zhang, and K. Wang, "Cogging torque optimization of flux memory pole-changing permanent magnet machine," *IEEE Trans. Appl. Supercond.*, vol. 26, no. 4, pp. 0603105, Jun. 2016.

[38] C. Yu and K. T. Chau, "Design, analysis, and control of DC-excited memory motors," *IEEE Trans. Energy Convers.*, vol. 26, no. 2, pp. 479-489, Jun. 2011.

[39] X. Zhu, Z. Xiang, L. Quan, W. Wu, and Y. Du, "Multimode optimization design methodology for a flux-controllable stator permanent magnet memory motor considering driving cycles," *IEEE Trans. Ind. Electron.*, vol. 65, no. 7, pp. 5353-5366, Jul. 2018.

[40] W. Li, K. T. Chau, Y. Gong, J. Z. Jiang, and F. Li, "A new flux-mnemonic dual-magnet brushless machine," *IEEE Trans. Magn.*, vol. 47, no. 10, pp. 4223-4226, Oct. 2011.

[41] C. Yu and K. T. Chau, "Dual-mode operation of DC-excited memory motors under flux regulation," *IEEE Trans. Ind. Appl.*, vol. 47, no. 5, pp. 2031-2041, Sep./Oct. 2011.

[42] Y. Gong, K. T. Chau, J. Z. Jiang, C. Yu, and W. Li, "Analysis of doubly salient memory motors using Preisach theory," *IEEE Trans. Magn.*, vol. 45, no. 10, pp. 4676-4679, Oct. 2009.

[43] W. Cui, Y. Gong, J. Jiang, and Y. Zhang, "Optimized doubly salient memory motors with symmetric features using transposition design methods," in *Proc. Int. Conf. Power Eng., Energy Electr. Drives (POWERENG)*, Malaga, Spain, 2011, pp. 1-7.

[44] F. Li, K. T. Chau, C. Liu, and Z. Zhen, "Design principles of permanent magnet dual-memory machines," *IEEE Trans. Magn.*, vol. 48, pp. 3234-3237, Nov. 2012.

[45] F. Li, K. T. Chau, C. Liu, J. Z. Jiang, and W. Yong, "Design and analysis of magnet proportioning for dual-memory machines," *IEEE Trans. Appl. Supercond.*, vol. 22, no. , pp. 4905404-4905404, Jun. 2012.

[46] F. Li, K. T. Chau, C. Liu, and C. Qiu, "New approach for pole-changing with dual-memory machine," IEEE Trans. Appl. Supercond., vol. 24, no. 3, Jun. 2014, Art. no. 0501504

[47] H. Yang, H. Lin, E. Zhuang, S. Fang, and Y. Huang, "Investigation of design methodology for non-rare-earth variable-flux switched flux memory machines," *IET Electr. Power Appl.*, vol. 10, no. 8, pp. 744-756, Sep. 2016.

[48] H. Yang, Z. Q. Zhu, H. Lin, D. Wu, H. Hua, S. Fang, and Y. Huang, "Novel high-performance switched flux hybrid magnet memory machines with reduced rare-earth magnets," *IEEE Trans. Ind. Appl.*, vol. 52, no. 5, pp. 3901-3915, Sept./Oct. 2014.

[49] H. Yang, H. Lin, Z. Q. Zhu, D. Wang, S. Fang, and Y. Huang, "A variable-flux hybrid-PM switched-flux memory machine for EV/HEV applications," *IEEE Trans. Ind. Appl.*, vol. 52, no. 3, pp. 2203-2214, May/Jun. 2014.

[50] H. Yang, H. Lin, S. Fang, Z. Q. Zhu, and Y. Huang, "Flux-regulatable characteristics analysis of a novel switched-flux surface-mounted PM memory machine," *IEEE Trans. Magn*., vol. 50, no. 11, Article No. 8103904, Dec. 2014.

[51] H. Yang, H. Lin, J. Dong, J. Yan, Y. Huang, and S. Fang, "Analysis of a novel switched-flux memory motor employing a time-divisional magnetization strategy," *IEEE Trans. Magn.*, vol. 50, no. 2, pp. 849-852, Feb. 2014.

[52] D. Wu, X. Liu, Z. Q. Zhu, A. Pride, R. Deodhar, T. Sasaki, "Novel switched-flux hybrid magnet memory motor," in *Proc. 7th IET Int. Conf. Power Electron. Machin. Drives, (PEMD),* Manchester, UK. 2014.

[53] X. Liu, D. Wu, Z. Q. Zhu, A. Pride, R. Deodhar, T. Sasaki, W. Q. Chu, "Efficiency improvement of memory switched flux PM machine over interior permanent magnet machine for EV/HEV applications," *IEEE Trans. Magn.* vol. 50, no. 11, Art. No: 8202104, Nov. 2014.

[54] H. Yang, Z. Q. Zhu, H. Lin, P. L. Xu, H. L. Zhan, S. Fang, and Y. Huang, "Design synthesis of switched flux hybrid-permanent magnet memory machines," *IEEE Trans. Energy Convers.*, vol. 32, no.1, pp. 65-79, Mar. 2017.

[55] L. Qin, H. Lin, H. Yang, H. Ni, D. Wang, K. Guo, and X. Lu, "Electromagnetic analysis of a novel axial-field switched flux hybrid magnet memory machine," in *Proc. 2016 Eleventh International Conference on Ecological Vehicles and Renewable Energies (EVER),* Monaco*,* 2016, pp. 1-6.

[56] N. Li, M. Lin, G. Yang, and L. Xu, "Design and analysis of a hybrid permanent magnet axial field flux-switching memory machine," *in Proc. 2016 IEEE Conference on Electromagnetic Field Computation (CEFC)*, Miami, 2016, pp. 1-1.

[57] H. Yang, Z. Q. Zhu, H. Lin, H. L. Zhan, H. Hua, E. Zhuang, S. Fang, and Y. Huang, "Hybrid-excited switched flux hybrid magnet memory machines," *IEEE Trans. Magn.*, vol. 52, no. 6, Article No. 8202215, Dec. 2015.

[58] H. Yang, H. Lin, Z. Q. Zhu, S. Fang, and Y. Huang, "A winding-switching concept for flux weakening in consequent magnet pole switched flux memory machine," *IEEE Trans. Magn.*, vol. 51, no. 11, Article No. 8108004, May 2015.

[59] H. Yang, H. Lin, Z. Q. Zhu, E. Zhuang, S. Fang, Y. Huang, "Operating-envelop-expandable control strategy for switched flux hybrid magnet memory machine," in *Proc. Energy Convers. Congr. and Expo. (ECCE), 2016 IEEE*, Milwaukee, U.S., 2016, pp. 1-8.

[60] H. Yang, Z. Q. Zhu, H. Lin, H. L. Zhan, H. Hua, E. Er, S. Fang, and Y. Huang, "Hybrid-excited switched flux hybrid memory machines," *IEEE Trans. Magn.*, vol. 52, no. 6, Article No. 8202215, Jun. 2016.

[61] X. Liu, D. Wu, Z. Q. Zhu, A. Pride, R. P. Deodhar, and T. Sasaki, "Efficiency improvement of switched flux PM memory machine over interior PM machine for EV/HEV applications," *IEEE Trans. Magn.*, vol. 50, no. 11, pp. 1106-1109, Nov. 2014.

[62] H. Yang, S. Lyu, H. Lin, and Z. Q. Zhu, "A variable-mode stator consequent pole memory machine," *AIP Advances*, vol. 8, no. 5, Article No. 056612, 2018.

[63] H. Yang, H. Lin, Z. Q. Zhu, S. Fang, and Y. Huang, A novel stator-consequent-pole memory machine, in *Proc. Energy Convers. Congr. and Expo. (ECCE), 2016 IEEE*, Milwaukee, U.S., 2016, pp. 1-8.

[64] H. Yang, H. Lin, Z. Q. Zhu, H. Wang, S. Fang, and Y. Huang, "A novel flux-reversal hybrid magnet memory machine," in *Proc. IEEE Energy Convers. Congr. Expo. (ECCE)*, Cincinnati, OH, Oct. 1-5, 2017, pp. 5853-5860.

[65] H. Yang, Z. Q. Zhu, H. Lin, and S. Lyu, "Novel variable reluctance hybrid magnet memory machines," *in Proc. 20th International Conference on Electrical Machines and Systems, ICEMS 2017*, Sydney, NSW, Australia, Aug. 11-14, 2017, No. 17239911.

[66] L. Jian, Y. Gong, J. Wei, Y. Shi, Z. Shao, and T. W. Ching, "A novel claw pole memory machine for wide-speed-range applications," *Journal of Applied Physics*, vol. 117, no. 17, Article No. 17A725, 2015.

[67] K. Sakai, H. Hashimoto, and S. Kuramochi, "Principle of hybrid variable-magnetic-force motors," in *Proc. Int. Electr. Mach. Drives Conf. (IEMDC)*, Niagara Fall[67]s, ON, 2011, pp. 53-58.

[68] H. Yang, H. Lin, Z. Q. Zhu, S. Fang, and Y. Huang, "A novel stator-consequent-pole memory machine," in *Proc. Energy Convers. Congr. and Expo. (ECCE), 2016 IEEE*, Milwaukee, U.S., 2016, pp. 1-8.

[69] H. Yang, H. Lin, Z. Q. Zhu, S. Fang, and Y. Huang, "A novel dual-layer PM variable flux hybrid memory machine," in *Proc. Energy Convers.*

Congr. and Expo. (ECCE), 2018 IEEE, Potland, U.S., 2018, submitted.
[70] Hui Yang, Z. Q. Zhu, Heyun Lin, Shuhua Fang, and Yunkai Huang, "Synthesis of hybrid magnet memory machines having separate stators for traction applications," *IEEE Trans. Veh. Technol.*, vol. 67, no. 1, pp. 183-195, Oct. 2017.
[71] H. Yang, Z. Q. Zhu, H. Lin, H. L. Zhan, H. Hua, E. Er, S. Fang, and Y. Huang, "Hybrid-excited switched flux hybrid memory machines," *IEEE Trans. Magn.*, vol. 52, no. 6, Article. 8202215, Jun. 2016.
[72] H. Yang, Z. Q. Zhu, H. Lin, Y. Zhang, S. Fang, Y. Huang, and N. Feng, "Performance improvement of partitioned stator switched flux memory machines with triple-magnet configuration," *IEEE Trans. Magn.*, vol. 52, no. 7, Article. 8104604, Jul. 2016.
[73] H. Yang, Z. Q. Zhu, H. Lin, K. Guo, Y. Guo, S. Fang, and Y. Huang. "Analysis of on-load magnetization characteristics in a novel partitioned stator hybrid magnet memory machine," *IEEE Trans. Magn.*, vol. 53, no. 6, Art. No. 8103404, Jan. 2017.
[74] H. Yang, H. Lin, Z. Q. Zhu, S. Fang, Y. Huang, and Z. Xu. "Novel variable-mode partitioned stator switched flux memory machines for automotive traction applications," *in Proc. 2016 XXII International Conference on Electrical Machines (ICEM)*. IEEE, 2016, pp: 844-850.
[75] H. Yang, H. Lin, Z. Q. Zhu, S. Fang, and Y. Huang, "A dual-consequent-pole vernier memory machine," *Energies*, vol. 9, no. 3, Article No. 134, Feb. 2016.
[76] Z. Q. Zhu, W. Q. Chu, and Y. Guan, "Quantitative comparison of electromagnetic performance of electrical machines for HEVs/EVs," *CES Trans. Electr. Machin. and Syst.*, vol. 1, no. 1, pp. 37-47, Mar. 2017.
[77] T. A. Burress, et al. "Evaluation of the 2010 Toyota Prius hybrid synergy drive system," Oak Ridge Nat. Lab., Oak Ridge, TN, USA, Tech. Rep. ORNL/TM-2010/253, Mar. 2011.

Hui Yang was born in Changning, Hunan Province, China. He received the B. Eng. degree from Dalian University of Technology, Dalian, China in 2011, and the Ph.D. degree from Southeast University, Nanjing, China in 2016, respectively, all in electrical engineering. From 2014 to 2015, he was supported by the China Scholarship Council through a one-year joint Ph.D. studentship at The University of Sheffield, Sheffield, U.K. Since 2016, Dr. Yang has been with Southeast University, where he has been a lecturer of School of Electrical Engineering. His research interests include design and analysis of novel permanent-magnet machines with particular reference to variable-flux machines for electric vehicles and renewable energy applications. He is the recipient of Best Paper Awards in ICEMS 2014 and EVER 2015, and the holder of 11 patents.

Heyun Lin obtained his B. S., M. S. and Ph. D. degrees in electrical engineering from Nanjing University of Aeronautics and Astronautics, Nanjing, P. R. China, in 1985, 1989 and 1992 respectively. From 1992 to 1994, he worked as a postdoctoral fellow in Southeast University, Nanjing, P. R. China. In 1994, he joined the School of Electrical Engineering, Southeast University as an Associate Professor and became a full Professor since 2000. His main research is related to the design, analysis and control of permanent magnet motor, intelligent electrical apparatus and electromagnetic field numerical analysis. He is the author of more than 150 technical papers and the holder of 30 patents. Prof. Lin is a Fellow of IET and a Senior Member of IEEE, who is also a member of Electrical Motor and Apparatus Committee of Jiangsu Province, and senior member of both China Society of Electrical Engineering and China Electrotechnical Society.

Z. Q. Zhu received the B. Eng. and M. Sc. degrees in electrical and electronic engineering from Zhejiang University, Hangzhou, China, in 1982 and 1984, respectively, and the Ph. D. degree in electrical and electronic engineering from The University of Sheffield, Sheffield, U.K., in 1991. Since 1988, he has been with The University of Sheffield, where he is currently a Professor with the Department of Electronic and Electrical Engineering, Head of the Electrical Machines and Drives Research Group, Royal Academy of Engineering/Siemens Research Chair, Academic Director of Sheffield Siemens Wind Power Research Centre, Director of Sheffield CRRC Electric Drives Technology Research Centre. His current major research interests include the design and control of permanent-magnet brushless machines and drives for applications ranging from automotive to renewable energy. He is a Fellow of Royal Academy of Engineering, U.K.